LUND UNIVERSITY

Modelling and Quality Assessment of Atrial Fibrillatory Waves

Henriksson, Mikael

2019

Document Version:
Publisher's PDF, also known as Version of record

Link to publication

Citation for published version (APA):
Henriksson, M. (2019). *Modelling and Quality Assessment of Atrial Fibrillatory Waves*. Department of Biomedical Engineering, Lund university.

Total number of authors:
1

Modelling and Quality Assessment of Atrial Fibrillatory Waves

Mikael Henriksson

Contents

Populärvetenskaplig Sammanfattning

Denna avhandling kretsar kring *förmaksflimmer*, en av våra vanligaste hjärtsjukdomar. Förmaksflimmer betraktas i regel inte som livshotande, men anses kunna leda till värre sjukdomar, i synnerhet stroke. Forskning rörande förmaksflimrets mekanismer motiveras alltså dels av att lindra symptomen, men även av att utveckla metoder att identifiera patienter så att åtgärder mot stroke kan sättas in i tid. Detta arbete tar sig an signalbehandling av EKG-signaler, elektriska hjärtsignaler inspelade från kroppsytan, och syftar till att utveckla analysmetoder som är robusta och tar fysiologiska och teknologiska begränsningar i beaktning.

Ett friskt hjärta styrs av sinusknutan i hjärtats högra förmak, som skickar elektriska impulser ner till kamrarna, vilka kontraherar och pumpar ut blod i kroppen, ett "hjärtslag". Under förmaksflimmer är detta system satt ur spel, då den oordnade elektriska aktiviteten i förmaken leder till en oregelbunden hjärtrytm. EKG-signaler domineras av den elektriska aktiviteten i kamrarna, och analysen baseras ofta endast på hjärtrytmen. Signalerna innehåller dock även den elektriska aktivitet i förmaken, vilket för patienter med förmaksflimmer innebär *flimmervågor*, vars upprepning, storlek och regelbundenhet varierar kraftigt mellan olika patienter. Flera studier av flimmervågor har funnit att deras egenskaper kan ge en indikation på hur patienten kommer att reagera på olika läkemedel, eller på kirurgisk behandling.

Utmaningen med att analysera flimmervågor består dels av att vågorna i viss mån döljs bakom den mer dominanta kammaraktiviteten, dels av att deras signalstyrka är förhållandevis låg. Det första problemet har behandlats grundligt under en längre tid, och det existerar numera flera metoder som med goda resultat filtrerar bort kammaraktiviteten från EKG-signalerna så att "rena" flimmervågor tillhandahålls. Problemet med låg signalstyrka har dock ofta förbisetts. Detta gör flimmervågsanalys väldigt

känslig för störningar, orsakade av, t.ex., elektroder som sitter lösa, eller elektrisk aktivitet från muskler.

Centrala teman i denna avhandling är modellering och signalkvalitet, samt de begränsningar låg signalkvalitet innebär för tillförlitligheten av flimmervågsanalys. Ett arbete presenterar en ny modell av AV-knutan, den delen av hjärtat som möjliggör överledning av elektriska impulser från förmaken till kamrarna. Modellen använder sig utav förhållandet mellan hjärtslagen och flimmervågornas dominanta frekvens för att uppskatta AV-knutans egenskaper på ett mer robust vis än tidigare metoder. Ett annat arbete använder sig av en flimmervågsmodell för att introducera ett nytt signalkvalitetsindex, speciellt utvecklat för flimmervågor. Detta index bedömer tillförlitligheten av analysen och höga indexvärden visar sig dessutom indikera närvaro av flimmervågor, vilket utnyttjas för att förbättra prestandan hos en förmaksflimmerdetektor. Övriga arbeten kretsar kring flimmervågsanalys och använder sig utav signalkvalitetsindexet. En studie finner att flimmervågornas kvalitet försämras avsevärt under viss fysisk aktivitet, och en annan studie demonstrerar hur flimmervågornas dominanta frekvens minskar under isolering av lungvenerna, en vanlig behandlingsmetod för förmaksflimmer. Det sista arbetet undersöker hur olika flimmervågsparametrar varierar inom och mellan olika patienter.

Abstract

This doctoral thesis revolves around the analysis of electrocardiogram (ECG) signals during atrial fibrillation (AF). Special emphasis is put on the atrial fibrillatory waves, sometimes called the f-waves, which is the ECG component reflecting the electrical activity of the atria.

The thesis comprises an introduction and five papers that introduce and apply methods on ECG-based analysis of AF. Paper I deals with modelling of the relationship between atrial and ventricular activity while papers II–V deal with the modeling, analysis and quality assessment of the f-waves, the atrial activity component of the ECG.

Paper I presents a novel statistical dual pathway model of the atrioventricular (AV) node during AF. The model accounts for pathway switching, meaning that atrial impulses may alternate between arriving at the slow and the fast pathway, even if the preceding impulse did not cause a ventricular activation. Comparison between the present model, defined by four parameters, and a reference model, defined by five parameters, does not reveal any difference in modelling capability. However, parameter estimates of the present model exhibit considerably lower variation, a finding that may be ascribed to the reduction of model parameters.

Paper II proposes an f-wave signal quality index (SQI). The SQI is computed using a harmonic f-wave model which allows for variation in frequency and amplitude. Unlike the noise level estimator used for comparison, the f-wave SQI reflects signal quality adequately also when the spectral content of the noise overlaps with that of the observed f-waves. The SQI is shown to be highly associated with f-wave presence, obtaining considerably smaller values when computed from non-AF signals, which is exploited to improve the performance of an AF detector.

Paper III investigates the signal quality aspects of 24h tracking of the dominant atrial frequency (DAF), using the f-wave SQI from Paper II. The use of the SQI reveals that 40% of all 5-s signal segments of the database should be excluded due to poor

quality, with the recordings of some patients being completely removed. Removal of the noisy segments reduced the variation of the DAF trend during both day- and night-time . A decrease in signal quality is observed during veloergometry exercise, with the quality restored immediately afterwards.

Paper IV investigates the f-wave changes occurring during pulmonary vein isolation, a treatment option for AF patients. Three f-wave parameters, derived from the harmonic f-wave model from Paper II, are included – the DAF, the f-wave amplitude, and a novel regularity parameter named the phase dispersion. All three f-wave parameters correlate with clinical characteristics, but none of them can predict AF recurrence. However, the DAF decreases significantly during the procedure.

Paper V investigates the reproducibility of f-wave parameters, including the three from paper IV as well as the spectral organization index and spatiotemporal variability, which have been included in previous studies on f-wave analysis. For each parameter, the variance ratio between the inter- and intrapatient variance, is computed, a larger ratio corresponding to better parameter stability and reproducibility. A substantial difference in inter- and intrapatient variation is found among different parameters, with the DAF and f-wave amplitude obtaining considerably larger variance ratios than the rest.

In summary, this thesis presents and evaluates tools for ECG-based AF analysis with special attention on robustness and quality control. The SQI presented in Paper II is applied in Paper III–V, and it is concluded that some kind of quality assessment should be considered in all future studies involving f-wave analysis.

List of Publications

Included

The dissertation comprises an introduction and five parts describing advances in non-invasive analysis of atrial fibrillation. The five parts are based on the following studies:

[1] Mikael Henriksson, Valentina D. A. Corino, Leif Sörnmo and Frida Sandberg, "A Statistical Atrioventricular Node Model Accounting for Pathway Switching During Atrial Fibrillation", in *IEEE Transactions on Biomedical Engineering*, vol. 63, no. 9, pp. 1842–1849, 2016.

Author's contribution
The author wrote the mathematical description of the model, designed and performed the experiments, and did most of the writing.

[2] Mikael Henriksson, Andrius Petrėnas, Vaidotas Marozas, Frida Sandberg and Leif Sörnmo, "Model-based Assessment of f-wave Signal Quality in Patients with Atrial Fibrillation", in *IEEE Transactions on Biomedical Engineering*, vol. 65, no. 11, pp. 2600–2611, 2018.

Author's contribution
The author developed the method, designed and performed the experiments, and did most of the writing.

[3] Birutė Paliakaitė, Andrius Petrėnas, Mikael Henriksson, Jurgita Skibarkienė, Raimondas Kubilius, Leif Sörnmo and Vaidotas Marozas, "Atrial Fibrillation Frequency Tracking in Ambulatory ECG Signals: The Significance of Signal Quality Assessment", in *Computers in Biology and Medicine*, vol. 102, pp. 227–233, 2018.

Author's contribution
The author developed the code for signal quality assessment and wrote part of the method description, as well as assisted in the design of some of the experiments.

[4] Mikael Henriksson, Arcadi García-Alberola, Rebeca Goya, Alba Vadillo, Francisco-Manuel Melgarejo-Meseguer, Frida Sandberg and Leif Sörnmo, "Changes in f-wave Characteristics during Cryoballoon Catheter Ablation", in *Physiological Measurements*, vol. 39, no. 10, pp. 105001, 2018.

Author's contribution
The author collected and processed the raw data used in this study, designed and performed the experiments, and did most of the writing.

[5] Mikael Henriksson and Leif Sörnmo, "Reproducibility of parameters characterizing atrial fibrillatory waves', Manuscript.

Author's contribution
The author came up with the idea, designed and performed the experiments, and did most of the writing.

Related

The related papers listed below are not included in the thesis.

[5] Mikael Henriksson, Valentina D. A. Corino, Leif Sörnmo and Frida Sandberg, "A novel statistical model of the dual pathway atrioventricular node during atrial fibrillation", *42nd Computing in Cardiology Conference (CinC)*, Nice, France, September, 2015.

[6] Mikael Henriksson, Andrius Petrėnas, Vaidotas Marozas, Frida Sandberg and Leif Sörnmo, "Signal Quality Assessment of f-waves in Atrial Fibrillation", *44nd Computing in Cardiology Conference (CinC)*, Rennes, France, September, 2017.

[7] Leif Sörnmo, Andrius Petrėnas, Mikael Henriksson and Vaidotas Marozas, "Letter regarding the article "Detecting atrial fibrillation by deep convolutional neural networks" by Xia et al.", in *Computers in Biology and Medicine*, vol. 100, pp. 41–42, 2018.

Acknowledgments

Several people have contributed to this thesis and deserve to be mentioned.

The first name is of course my supervisor Leif, for being supportive, principled, and an expert within this field. His scientific vision permeates all of this work, and it is fair to say that it greatly influences his PhD students as well. My co-supervisor Frida has also contributed with considerable time and effort.

All included papers are products of international collaborations. I want to give special attention to the group in Kaunas (Vaidotas, Andrius, Birutė) that I authored two papers with and that hosted me during my visit in Lithuania. Also, Arcadi provided invaluable guidance and assistance, and was a great host, during my visit in Murcia, Spain.

Another mention goes to all the members of the biomedical signal processing group, past and present, with a very special mention to Hamid, my office comrade during most of my time here. Additionally, all other colleagues at the department of Biomedical Engineering deserve praise for creating such a pleasant work environment. Finally, on the inevitable personal note…

Min familj och mina vänner påminner mig ständigt om vad som verkligen betyder något här i livet. Denna insikt hjälper mig att studera och arbeta med ett stoiskt lugn, utan stress och utan att nedslås av motgångar. Tack till er alla.

<div align="right">

Mikael Allan Einar Henriksson
Lund, New Year's Day 2019

</div>

Introduction

Chapter 1
Motivation and Background

This thesis deals with the analysis of atrial fibrillation (AF) from electrocardiogram (ECG) signals, measured non-invasively from the body surface. The increasing prevalence of AF demonstrates the need for reliable screening and diagnosis, where large amounts of data may need to be automatically classified. Also, many aspects of the disease remain unclear, which motivate the development of research tools that provide ways to identify AF properties.

The common theme of all included papers is the analysis of atrial fibrillatory waves, sometimes called *f-waves*, which is the atrial component of the ECG. Special consideration is given to signal quality. All papers involve classifying subsets of signals or estimates as unreliable, and consequently removing them from further analysis. The thesis sets out to investigate the boundaries of ECG-based AF analysis, and shed some light on what can be expected from current measurement techniques.

The work presented in this thesis consists of five parts.

- Paper I presents a novel model of the atrioventricular (AV) nodal function during AF, enabling robust estimation of multiple AV nodal parameters.

- Paper II presents a novel index for assessment of f-wave signal quality, and investigates its significance in frequency estimation and AF detection.

- Paper III studies frequency tracking in long-term ambulatory ECG recordings, applying the signal quality index from Paper II.

- Paper IV investigates the changes in f-wave parameters occurring during isolation of the pulmonary veins.

- Paper V studies the reproducibility of several f-wave parameters.

The remainder of this introductory chapter presents a general overview of the human heart (Sec. 1.1) and AF (Sec. 1.2), including treatment options. Chapter 2 deals with the basics of ECG signal processing and presents various types of analysis using only ventricular information (Sec. 2.1), ways to determine the quality of ECG signals (Sec. 2.2), and mathematical models of the AV node (Sec. 2.3). Chapter 3 deals with f-waves, including ways to extract (Sec. 3.1) and to model (Sec. 3.2) them. Section 3.3 introduces several parameters used to characterize the f-waves as well as their use in AF detection, while Sec. 3.4 discusses the influence of noisy on f-wave analysis—a central theme of this thesis. Finally, summaries of the five included papers are presented in Ch. 4.

1.1   The human heart

The human heart consists of a right and a left part, each of which is made up of an atrium and a ventricle. The anatomy of the heart is illustrated in Fig. 1.1. During a cardiac cycle, the right atrium receives deoxygenated blood from the veins and pushes it to the right ventricle through the right AV valve. The right ventricle then contracts and the blood is pushed through the pulmonary artery to the lungs where it is oxygenated before entering the left atrium. The subsequent contraction of the left atrium lets the blood pass through the left AV valve to the left ventricle which finally contracts and pushes the oxygenated blood into the aorta which transports it to the organs of the body.

In a healthy heart, this process is coordinated by electrical impulses originating from the sinoatrial (SA) node located in the right atrium. The SA node, described as the natural pacemaker of the heart, generates electrical impulses at a rate modulated by the autonomic nervous system. Each impulse traverses the atria and causes the right and the left atrium to contract simultaneously. The impulse then enters the AV node, the part of the electrical conduction system of the heart which connects the atria and the ventricles. The conduction velocity of the impulse is slowed significantly in the AV node, causing a delay. When any part of the electrical conduction system of the heart, e.g. the AV node, is activated, its tissue gets depolarized and it needs to be repolarized before being activated again. During the repolarization, the tissue is said to be refractory. The refractory period of the AV node will therefore limit the heart rate, as two impulses arriving close to each other may not both be conducted to the ventricles. The shortest time interval between conducted impulses is referred to as the functional refractory period of the AV node. After passing through the AV node, the conduction velocity increases again as the impulse traverses the bundle of His and the Purkinje fibers before it causes both the left and the right ventricle to contract simultaneously. The delay of the impulse in the AV node causes a sufficient
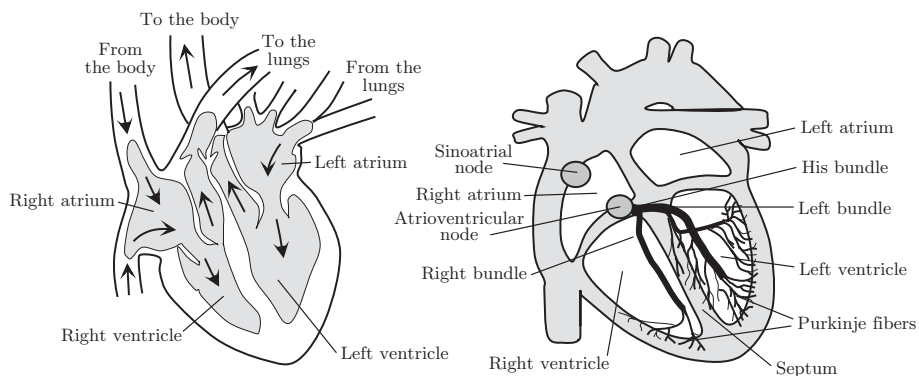
Figure 1.1: Anatomic overview of the heart. Reprinted with permission from [1].

time difference between the atrial contractions and the ventricular contractions to allow the ventricles to be filled with blood. The heart rate is consequently directly controlled by the rate of impulses from SA node, and this is referred to as normal sinus rhythm (SR).

1.2 Atrial fibrillation

Atrial fibrillation is the world's most common arrhythmia, characterized by rapid and irregular heart beats. Recent reports suggest an AF prevalence rate of approximately 3% in adults, a number which is expected to increase with an ageing population [2].

While the exact mechanisms of AF remain unknown, it is distinguished by electrical disorganisation in the atria, causing incomplete atrial contractions, and preventing the SA node from acting as the natural pacemaker of the heart during AF. The AV node is bombarded by electrical impulses in a seemingly uncoordinated manner which ultimately results in irregular ventricular contractions and, consequently, an irregular heart rhythm.

Atrial fibrillation is often classified into different AF types, including; paroxysmal AF, consisting of self-terminating episodes lasting no more than seven days; persistent AF, consisting of AF episodes failing to terminate within seven day; long-standing persistent AF, where AF has lasted more than one year; and permanent AF, where attempts to restore SR have been unsuccessful and the physician has accepted the presence of AF. The AF type is not considered to be static as, e.g., a paroxysmal AF patient may very well transition into persistent AF.

Atrial fibrillation may manifest itself in a variety of symptoms, most commonly palpitations and shortness of breath [3]. However, many patients suffering from AF

are symptom-free, suggesting an underestimation of AF prevalence. Atrial fibrillation is also associated with increased mortality, in particular by the increased risk of stroke. This since the incomplete contraction of the atria may cause blood to coagulate and form blood clots. Atrial fibrillation is therefore generally treated by prescribing anticoagulants medication to the patient. Restoration of SR can also be attempted by either pharmacological or electrical cardioversion. If the restoration to SR is unsuccessful, rate-control drugs can be used to control the heart rhythm.

1.2.1   Treatment

Apart from the admission of anticoagulants, AF management strategies can be classified into one of two options; rate control, which sets out to control the fast and irregular heart rate; and rhythm control, which is focused on preventing AF recurrence or restoring SR.

Rate control has been referred to as the therapy of choice for AF [4]. It commonly involves lowering the heart rate to at most 80 beats per minute at rest, typically by the use of pharmaceuticals such as beta-blockers or calcium-channel blockers. The drugs influences the properties of the AV node so that fewer atrial impulses are conducted, thus slowing down the heart rate. The electrical isolation of the AV node through the use of catheter ablation is another treatment option, although it is rarely performed due to the severity of the procedure as it leaves the subject completely pacemaker-dependent.

Rhythm control therapy may be attempted if a rate control approach has proven unsatisfactory, or if AF is at an early stage and the progression to persistent or permanent AF wants to be avoided. Restoration of SR may be attempted through the use of antiarrhythmic drugs or electrical cardioversion. Another approach is to isolate the pulmonary veins in the left atrium, being a frequent source of AF-inducing ectopic beats [5]. Catheter ablation is performed either by application of a radiofrequency current or a cryoballoon, with the former being the most common, although the cryoballoon has been suggested to be safer, simpler, and with similar clinical performance [6, 7, 8]. The outcome of catheter ablation is typically determined from whether AF is recurrent during follow-up studies, with worse outcome associated with the more advanced AF types [9, 10, 11]. For this reason, most catheter ablations are performed on paroxysmal AF patients [12]. The pulmonary vein isolation is often followed by an electrical cardioversion, or by additional ablation in the left or right atrium steps if considered necessary.

Chapter 2
ECG Signal Processing

The electrical activity of the heart can be measured in different ways, where the ECG is the arguably most accessible and widely studied approach. The original ECG technique was presented already in the 1880s and has since evolved to become the most common cardiological diagnostic test in clinical practice. The ECG is obtained from electrodes placed on the body surface and records variations in the electrical field caused by the electrical activity of the heart. The standard 12-lead ECG, using 10 electrodes, is the most commonly used ECG configuration, with six of the electrodes placed on the torso and four on the limbs. However, the standard 12-lead ECG is not optimized to obtain atrial information, since, historically, ECG analysis has mainly been focused on ventricular activity. Other lead configurations specifically designed to record atrial activity have been proposed [13, 14], although replacing the 12-lead configuration in a clinical setting has proven difficult since it is so widely used.

ECG recordings from lead V_1, which is the lead closest to the right atrium in the 12-lead configuration, are presented in Fig. 2.1. The large wave is denoted the *R-wave* and the region around it is referred to as the *QRS complex*. The QRS complex is caused by rapid depolarization of the ventricles preceding ventricular contraction. Repolarization of the ventricles is reflected by the wave following the QRS complex, called the T-wave. In Fig. 2.1(a), obtained from a patient in SR, the QRS complex is preceded by an impulse of smaller amplitude, which is called the *P-wave* and reflects atrial depolarizaton. Note that atrial repolarization is not visible in the ECG as it has too low amplitude and usually coincides with the QRS complex. An ECG recording from a patient with AF, illustrated in Fig. 2.1(b), no longer contains P-waves. Instead, irregular waves, reflecting the disorganization of the atria, is present. These f-waves are used in the analysis and characterization of AF. The separation of atrial and ventricular activity enables the analysis of f-waves, see Sec. 3.1.

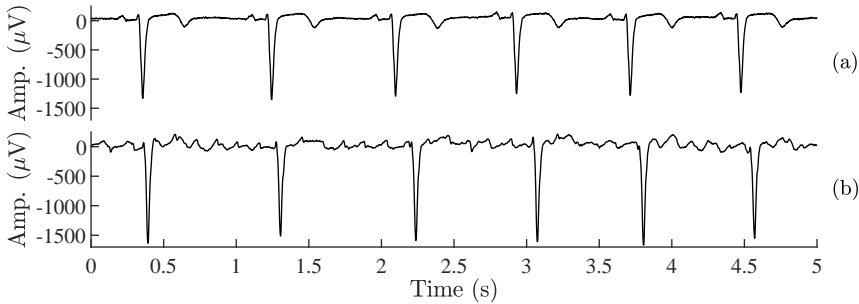When long-term ECG recordings are desired, the 12-lead configuration is no

Figure 2.1: Example of an ECG in lead V_1 record from a patient in (a) SR and (b) AF.

longer feasible. Instead, portable ECG recorders, often called Holter monitors, are being used. A three-lead configuration is usually applied, although many different variants exist. A subject wears the device during ordinary daily activities, and continuous signals are recorded during a period as long as one or two days. The quality of the recordings are usually considerably poorer than 12-lead ECG signals, mainly due to electrode motion and excessive muscle noise. Just like for 12-lead ECGs, Holter lead configurations which enhance the atrial activity have been proposed [15].

Handheld recorders constitute a special type of portable ECG devices. They only record one single lead by having the user press their hands or fingers against the device. Instead of recording one long continuous signal, the user records ECG signals in episodes ranging from 5–10 s to a couple of minutes. The recording procedure can be repeated several times per day if necessary, and potentially being sent to a web server for analysis. Handheld recorders have demonstrated great potential for AF screening [16], although problems remain with low signal quality and the need to manually review large amounts of data. Also, the options for atrial activity extraction are considerably more limited due to the lack of additional leads.

Other lead systems or recording devices, not further studied in this thesis, include body surface potential maps, where a large number of electrodes are placed on the body surface to enable enhanced spatial resolution. Wearable ECG monitoring systems, with textile-based sensors, is also an emerging field [17], as is the use of small biopatches [18]. Localized electrical activity can be provided by electrogram recordings, obtained from intracardiac (i.e. inside the heart) electrodes. Since electrograms are recorded invasively, they are not a realistic alternative for wide use because of the cost and risk involved.

2.1 Characterization of ventricular response

When no atrial information is directly available, for example when the signal quality does not allow for the extraction and analysis of f-waves, evaluation of AF has to be accomplished using only the ventricular response which constitutes the dominant part of the ECG. Contrary to when in SR, in which the ventricular response typically is regular, the ventricular response during AF is more chaotic with some studies suggesting it as being random in the short-term [19]. However, other studies suggested deterministic attributes and related weak short-term predictability, leaving the matter unsettled for the time being [20].

Analysis of the ventricular response is typically performed using the RR interval series, sometimes referred to the interval tachogram, $d_{\mathrm{RR}}(k)$, computed from the detected QRS complexes ,

$$d_{\mathrm{RR}}(k) = t_k - t_{k-1}, \quad k = 1, \dots, N_d \tag{2.1}$$

where N_d is to total number of detected QRS complexes and t_k denotes the timing of the k:th R-wave. Several methods for analysis of the RR interval series have been proposed and used to assess, e.g., the properties of the AV node [21] and the effect of drugs [22]. A major limitation of this analysis is the requirement of long windows of data, commonly several minutes long, making the analysis of short variations unfeasible.

2.1.1 RR interval histogram analysis

The RR interval series $d_{\mathrm{RR}}(k)$ may be presented as a histogram. For SR, a sharp peak is typically present, indicating a regular heart rhythm as the timing between consecutive heart beats is relative constant, see Fig. 2.2(a). For AF, the histogram is typically smeared out, illustrating the irregular heart rhythm, see Fig. 2.2(b). Also, in many AF patients, two or more distinct peaks are present. One study found bimodal RR interval histograms in 55% of the patients [23]. Another study found a significant correlation between bimodal RR interval histograms and early recurrence of AF after electrical cardioversion [24]. The presence of bimodal RR interval histogram is also widely considered to indicate the presence of dual pathways in the AV node [25].
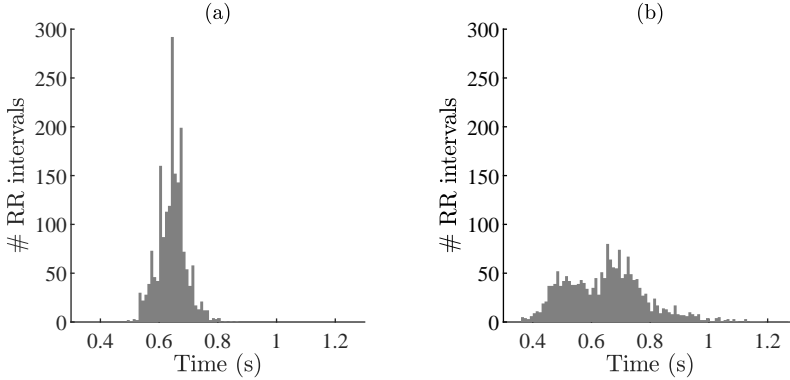
Figure 2.2: RR interval histograms from 20 min ECG recordings of; (a) a SR patient, from the PTB Diagnostic ECG Database [26]; and (b) an AF patient, from the RATAF database [27].

2.1.2   Variability and irregularity parameters

The variability and irregularity of d_{RR} can be quantified by a number of different parameters, which have been used to classify or describe AF. Common variability measures include the *coefficient of variation* V_{CV}, defined as the standard deviation divided by the mean, and the *root mean square of successive differences* V_{RMSSD} [28], defined as

$$V_{\text{RMSSD}} = \sqrt{\frac{1}{N_d} \sum_{n=1}^{N_d-1} d_{\text{RR}}^2(k)}. \tag{2.2}$$

Irregularity is often described by measures such as the *sample entropy*, I_{SampEn}, which was introduced in [29] and has, among other things, been shown to be indicative of the onset of paroxysmal AF [30]. It is defined as

$$I_{\text{SampEn}}(m, r) = \ln\left(\frac{B(m, r)}{B(m+1, r)}\right) \tag{2.3}$$

where $B(m, r)$ denotes the estimated probability that a signal segment of length m will repeat itself, with r defining the required degree of similarity. It is computed as

$$B(m, r) = \frac{1}{(N_d - m)(N_d - m - 1)} \sum_{i=1}^{N_d-m} \sum_{j=1, j \neq i}^{N_d-m} H\left(r - ||\mathbf{d}_{\text{RR}}^m(i) - \mathbf{d}_{\text{RR}}^m(j)||_\infty\right),$$
$$\tag{2.4}$$

where $H(.)$ denotes the Heaviside step function and $||.||_\infty$ denotes the infinity norm. The vector $\mathbf{d}_{\mathrm{RR}}^m(i)$ consists of m RR intervals, starting at $d_{\mathrm{RR}}(i)$. For a regular signal, $B(m+1, r)$ obtains a value similar to $B(m, r)$, which corresponds to a low I_{SampEn}. However, an increase in I_{SampEn} corresponds to an increasingly irregular signal and serves as a predictor for the transition from SR to AF.

Another commonly used irregularity measure is the *Shannon entropy*, I_{ShEn}, computed using the estimated probability density function (PDF), $\hat{p}(k)$, of the signal. The PDF $\hat{p}(k)$ is typically obtained from the RR interval histogram, where $D(k)$ is the number of RR interval values in the k:th bin. The Shannon entropy is then computed as

$$I_{\mathrm{ShEn}} = -\sum_{k=1}^{K} \hat{p}(k) \log_2(\hat{p}(k)) = -\sum_{k=1}^{K} \frac{D(k)}{N_d} \log_2\left(\frac{D(k)}{N_d}\right) \qquad (2.5)$$

where K is the number of bins in the histogram.

A low or decreasing RR interval variability or irregularity in AF has been associated with increased mortality [31, 32]. Rate-control drugs have been found to increase RR interval variability [22, 33, 34]. Another use of variability and irregularity measures is to separate AF recordings from non-AF recordings, which is the topic of the next section.

2.1.3 Detection of AF using the RR interval series

As mentioned earlier, one of the main characteristics of AF is the irregular heart rhythm. Therefore, AF detection methods operating on $d_{\mathrm{RR}}(k)$, commonly referred to as rhythm-based AF detectors, constitute the by far most common detection approach. A great advantage of these methods is their ability to function in relatively noisy or low-resolution environments, such as recordings from handheld ECG devices. The limitations of rhythm-based AF detectors are mainly the challenge of distinguishing between AF and non-AF arrhythmias, as well as the need of long signals to provide a sufficient number of RR intervals for analysis, rendering it difficult to detect very short AF episodes. Ectopic beats may constitute a problem as they can cause false detections, an issue which some rhythm-based detectors acknowledge by excluding RR intervals if their pattern resembles that of premature beats [36].

Rhythm-based AF detectors typically compute a metric from $d_{\mathrm{RR}}(k)$ which is then used to determine the presence of AF. The metric is often obtained from a sliding time window which enables detection of AF episodes. The length of the window varies between methods, but may be as short as 8 beats [35]. Many detectors make use of the measures described in Sec. 2.1.2, including V_{CV} [37], and irregularity metrics such as I_{ShEn} [38] or I_{SampEn} [39]. An extension of the sample entropy named
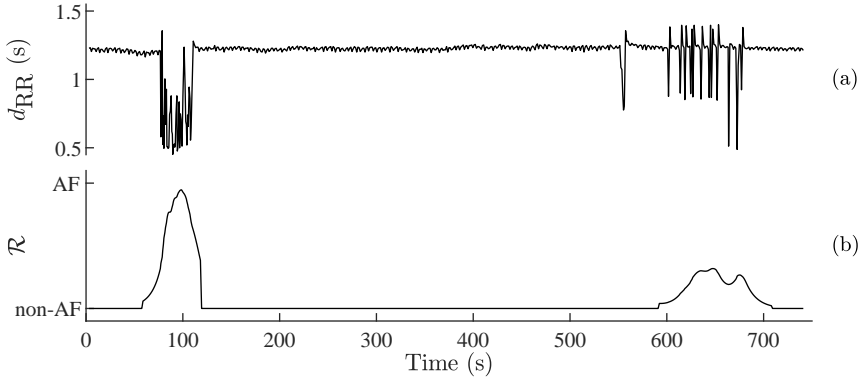
Figure 2.3: (a) The RR interval series $d_{RR}(k)$ of an paroxysmal AF patient and (b) the corresponding output of the rhythm-based AF detector $\mathcal{R}$ [35]. The detector correctly identifies one AF episode, however, the ectopic beats starting around 600 s also cause an increase in $\mathcal{R}$.

normalized fuzzy entropy, specifically developed for rhythm-based AF detection, has also been presented [40]. Other approaches to AF detection include RR interval histograms [41], Poincaré plots [42] and a time-varying coherence function [43].

All these methods rely upon correct beat detection, which may degrade in the presence of noise. In [44], the impact of added motion artefact noise on several different rhythm-based AF detection methods was studied. The results were relatively similar among all the studied methods as the number of false positive increases with increasing noise levels since many false detections are made. The study suggested a linear relationship between AF detection performance and SNR. It is thus highly recommended that signal quality assessment is incorporated in the detection method to ensure that the presence of muscle noise or motion artefacts does not cause correct detections.

An example of rhythm-based AF detection using the irregularity metric described in [35], $\mathcal{R}$, is presented in Fig. 2.3. Although an episode of paroxysmal AF is correctly identified, the detector output is also influenced by the non-AF arrhythmia. This influence can be reduced by including analysis of atrial activity in the detector, see Sec. 3.3.4.

The performance of an AF detector is typically evaluated using an annotated database, where the annotator output defines the gold standard. One of the databases frequently used for this purpose is the MIT-BIH AF database (AFDB) from Physionet [45, 46], which contains recordings of 25 AF patients.

2.2   Signal quality considerations

The ECG signal may be corrupted by noise from several different sources. While some disturbances, such as baseline wander or power line interference, typically can be removed by linear filtering, others, such as those originating from muscle activity or electrode movements, may overlap spectrally with the content of the ECG signal, thereby being considerably more difficult to remove which may cause the signal to be unusable for certain types of analysis [1]. A variety of algorithms designed to remove artifacts from the signals have been developed, but there is currently no gold standard method and the research field is considered to be open [47]. The assessment of signal quality is therefore of great importance when determining the reliability of the results from ECG analysis.

One of the most important applications of ECG signal quality assessment is to determine whether the detection is reliable. False beat detections seriously impair the reliability of RR interval analysis and could cause false alarms, which has been identified as a problem associated with patients under surveillance [48]. A number of studies from intensive care units have found that less than 10% of the alarms are of clinical importance [49, 50, 51]. Other applications of signal quality assessment include evaluation of recordings obtained in mHealth environments [52], where it is essential to exclude noisy data from further analysis without having to manually review the data.

Many proposed signal quality assessment methods rely on computations of a number of metrics which are then combined to define a signal quality index (SQI) of the signal [53, 54, 55, 56]. Typical metrics are the kurtosis, the agreement between outputs of beat detectors with different sensitivity and the relative power in the frequency range expected to contain the QRS complex. All these metrics are expected to attain large values for signals without noise. A machine learning algorithm is then applied to a training set in order to define the weights which will be applied to all the signal quality metrics in order to compute the final SQI. A limitation of this approach, typical of machine learning methods, is the need for large annotated training datasets which contain sufficient representations of many different patients and rhythms.

Examples of other metrics include those based directly on $d_{\mathrm{RR}}(k)$ itself [57], or on the similarity of the signal segment surrounding the R-wave [58], neither approach being feasible when assessing the quality of AF recordings. Signal quality assessment of ECG signals can be considered a growing research field, and several review articles have been written on the subject [59, 60].

2.3   AV node modelling

Contrary to when in SR, the main determinant of the ventricular response during AF is no longer the SA node but rather the AV node in combination with the atrial activity, see Sec. 1.1. The AV node, described by its characteristics and functionality such as dual pathways, concealed conduction and refractoriness, has been modelled in a variety of ways. This section describes some of the advances in modelling of the AV nodal function during AF.

2.3.1   Modeling of atrial activations series

When modeling the AV nodal function during AF, simulated atrial activations (AA) are needed. This is often accomplished by simulation, commonly involving a Poisson process [61, 62, 63, 64, 65]. The Poisson process is a practical choice because of its rigid mathematical description and the fact that it is defined solely by one variable, the arrival rate of its impulses. This means that the time interval between two atrial impulses is exponentially distributed and the there are a lack of statistical dependences between impulses.

   However, the Gaussian distribution has also been used to define the timing between two atrial activations [66]. Comparisons between the Poisson distribution, the Gaussian distribution and the Type IV Pearson distribution found that the latter more accurately captured the statistical properties of real AA series and therefore suggested as an alternative to the Poisson distribution when evaluating the AV node and its influence of the ventricular response [67].

   Some studies on the AV node involve using recordings of AA series. In [68], electrogram recordings from the right atrium are obtained from a patient with permanent AF. The AA series is then determined by identifying the atrial activation times from the recording.

2.3.2   Dynamic modelling of the AV node

In [68], a dynamic model of the AV nodal function is presented which incorporates concealed conduction, i.e. when an incomplete conduction results in a prolonged refractory period, by increasing the default refractory time with a fixed amount for each atrial impulse arriving while the AV node is refractory. The refractory period is reset to its default value after each ventricular activation. The conduction time for the atrial impulse, c, is determined by the time interval Δt, defined as the time between the end of the last refractory period and the activation time of the current

atrial impulse,

$$c = c_{\min} + c_{\text{ext}} \exp\left[-\frac{\Delta t}{t_c}\right] \tag{2.6}$$

where $c_{\min}$ is the minimum conduction time, c_{ext} is the maximal extension of conduction time, and t_c is a time constant.

Another dynamic model, based on the model presented in [61], was originally described in [62] and later extended in [63] to include both atrial and ventricular pacing. The AV node is treated as one lumped structure and is described by parameters defining, for example, the resting potential of the AV node, the refractory period and the conduction delay. Designed to be used for simulations of RR intervals, the model is, because of its complexity, not suitable for model parameter estimation. The refractory period τ is defined as

$$\tau = \tau_{\min} + \tau_{\text{ext}} \left(1 - \exp\left[-\frac{\Delta t}{t_\tau}\right]\right), \tag{2.7}$$

where $\tau_{\min}$ is the minimum refractory period, τ_{ext} is the maximal extension of the refractory period, and t_τ is a time constant. To incorporate concealed conduction, a term is added to τ to define the prolonged refractory period τ',

$$\tau' = \tau + \tau_{\min} \left(\frac{\Delta t_B}{\tau}\right)^{\rho_1} \left(\max\left(1, \frac{\Delta V}{V_t - V_r}\right)\right)^{\rho_2}, \tag{2.8}$$

where Δt_B is the time interval between the end of the last refractory period and the activation time of the blocked atrial impulse, ρ_1 and ρ_2 are electrotonic modulation factors, V_r and V_t are the AV node's resting potential and depolarisation threshold, respectively, and ΔV is the increase in voltage created by each atrial impulse. An atrial impulse is conducted when the potential V_m exceeds the threshold V_t,

$$V_m = V_r + n_{\text{AA}}\Delta V + \dot{V}\Delta t_B \geq V_t, \tag{2.9}$$

where V_r is the resting potential, n_{AA} is the number of arrived atrial impulses and $\dot{V}$ is the spontaneous depolarisation rate. The conduction time is described as in (2.6), and neither of the models include dual pathways of the AV node.

Another approach to AV node modeling was presented in [69]. Instead of treating the AV node as one lumped structure, it is presented as a number of connected nodes, each with a conduction time and refractory period as defined by (2.6) and (2.7). In order for an atrial impulse to traverse the AV node, it consequently has to pass several separate nodes constituting one of the two pathways, making concealed conduction an intrinsic property of the model. Parameter estimation is performed by matching

the observed RR interval series to the simulated RR interval series obtained from 1000 different parameter sets, although it does not result in a unique set of AV node parameters.

A very detailed model of the AV node was proposed in [70]. The model is designed to simulate action potentials and is, because of its computational complexity, not suited for the simulation of RR intervals or the estimation of AV nodal properties.

2.3.3   Statistical modelling

Described in [64, 65], a statistical model of the AV node is designed to provide a realistic ventricular response from atrial activations while also being simple enough for ECG-based parameter estimation, thereby providing a non-invasive approach for estimation of AV nodal properties. A graphic presentation of the model is illustrated in Fig. 2.4.

The AV node is modelled with dual pathways defined by a total of five parameters. The parameter τ_1 corresponds to the minimum refractory period of the slow pathway, meaning that all atrial impulses arriving before τ_1 are blocked. The prolongation parameter $\tau_{p,1}$ defines the maximum time that the slow pathway can remain refractory after τ_1, meaning that no atrial impulses arriving after $\tau_1 + \tau_{p,1}$ are blocked. The likelihood of the slow pathway being refractory decreases at a linear rate, meaning that the probability of the slow pathway being refractory at the time t following a ventricular contraction, $\beta_1(t)$, can be formulated as

$$\beta_1(\Delta t) = \begin{cases} 0, & 0 \leq \Delta t \leq \tau_1 \\ \frac{\Delta t - \tau_1}{\tau_{1,p}}, & \tau_1 \leq \Delta t \leq \tau_1 + \tau_{1,p} \\ 1, & \tau_1 + \tau_{1,p} \leq \Delta t. \end{cases} \tag{2.10}$$

The function $\beta_2(\Delta t)$, describing the corresponding probability for the fast pathway, is
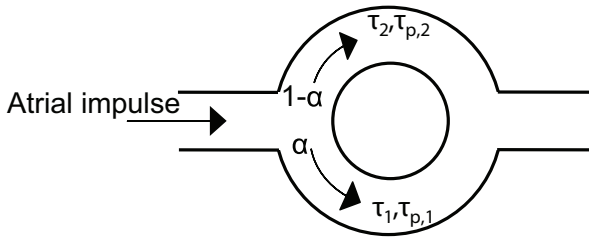

Figure 2.4: Modelling of the dual pathway AV node. Reprinted with permission from [65].

defined in a similar way using the minimum refractory time τ_2 and prolongation $\tau_{2,p}$. The minimum refractory period of the slow pathway is assumed to always be shorter than the minimum refractory period of the fast pathway, i.e. $\tau_1 < \tau_2$, meaning that τ_1 can be seen as an estimate of the functional refractory period. The parameter α defines the probability that an atrial impulse will be conducted through the slow pathway, thus influencing the bimodality of the RR histogram. Unlike previous models, an atrial impulse arriving at the AV node is always conducted unless the AV node is refractory. Neither the spontaneous depolarisation of the AV node nor the conduction time are featured in the model.

By assuming that the atrial activations arrive according to a Poisson process with an intensity defined by the estimated *dominant atrial frequency* (DAF), see Sec. 3.3.1, the model parameters can be obtained using maximum likelihood estimation (MLE) on recorded RR series. This approach to estimation has been applied on a number of studies to evaluate the effect of rate-control drugs during AF [71, 72, 73, 74].

The model presented in Paper I is also based on this statistical modelling approach [75]. To compensate for the observed overfitting of the previous models [64, 65], the number of estimated parameters is reduced by omitting α from the estimation. The value of α is instead computed and used as a measure of the reliability of the other parameter estimates.

Chapter 3

Analysis of Atrial Activity

3.1 Extraction of atrial activity

Since f-waves have far smaller amplitude than the QRS complexes, it is necessary to remove the ventricular activity if atrial information is to be studied. This is not feasible to accomplish by linear filtering since there is an overlap between the frequency content of the f-waves and the frequency content of the ventricular activity. Several different methods for atrial activity extraction, sometimes referred to as QRST cancellation, have been proposed and evaluated [76, 77]. This section describes atrial activity extraction methods based on average beat subtraction (ABS), independent component analysis (ICA), and adaptive filtering.

3.1.1 Average beat subtraction methods

Average beat subtraction methods constitute one of the most commonly used approaches for atrial activity extraction. The idea is that the QRS complex and the T-wave (referred to as the QRST complex in the following) are removed from the signal by subtraction of a template QRST complex $\bar{\mathbf{y}}$, created by averaging several QRST complexes in the signal. The averaging procedure is assumed to attenuate the f-waves since they are decoupled from the ventricular activity. The subtraction is preceded by beat detection and morphology grouping, as several different QRST complex morphologies may be present which requires different templates $\bar{\mathbf{y}}$. For each signal segment $\mathbf{y}$, containing one QRST complex, the corresponding $\bar{\mathbf{y}}$ is shifted τ_s samples using the shift matrix $\mathbf{J}_{\tau_s}$ to find the optimal fit.

A problem with the standard ABS approach is that the morphology of the QRST complex may be subjected to minor changes, primarily caused by movements of electrodes due to respiration. The fix QRST template will therefore not always be an
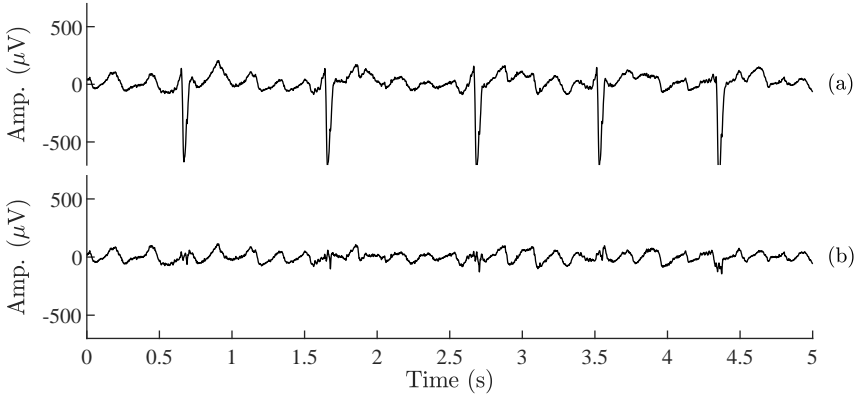
Figure 3.1: (a) ECG signal from lead V_1 before and (b) after spatiotemporal QRST cancellation.

optimal match. This is taken into account when using spatiotemporal QRST cancellation [78], where the signal segment **y** is replaced with the matrix **Y**, consisting of simultaneous recordings from multiple leads. The matrix $\bar{\mathbf{Y}}$, consisting of the QRST templates for all leads, is multiplied with the diagonal amplitude scaling matrix **D** and the rotation matrix **Q**. The minimization problem now becomes

$$\epsilon_{\min}^2 = \underset{\mathbf{D},\mathbf{Q},\tau_s}{\arg\min} \left\| \mathbf{Z} - \mathbf{J}_{\tau_s}\bar{\mathbf{Y}}\mathbf{D}\mathbf{Q} \right\|_F^2 , \qquad (3.1)$$

where $\|.\|_F^2$ denotes the Frobenius norm. Note that a grid search involving all variables is not feasible and the optimization is instead performed iteratively. Also, the matrix **Z**, defined as

$$\mathbf{Z} = \mathbf{Y} - \bar{\mathbf{Y}}_A \qquad (3.2)$$

is used instead of **Y**, where $\bar{\mathbf{Y}}_A$ is the intermediate fibrillation signal obtained from the segment between the T-wave and the subsequent QRS complex. This is to prevent the minimization in (3.1) from attenuating the f-waves. The result of spatiotemporal QRST cancellation on an ECG signal from an AF patient is illustrated in Fig. 3.1.

When dealing with ABS methods, problems may arise involving ectopic beats with morphologies differing from the QRST complexes. The removal of ectopic beats from the atrial signal may therefore be unsuccessful. A method has been developed which deals with the removal of ectopic beats prior to the atrial activity cancellation using principal component analysis [79]. In conclusion, ABS methods are robust, easy to implement, and also the only method described in this thesis applicable on single-lead ECG recordings. This makes ABS the most common and widely accepted

technique for atrial activity extraction. Spatiotemporal QRST cancellation is used to extract atrial activity in Papers I, II and V.

3.1.2   Independent component analysis

Signal separation by ICA is a general approach to separating different components in an observed signal. In ICA, it is assumed that the observed signal is a linear mix of a number of signals from independent sources. In [80], ICA was used to separate the atrial and ventricular signals, using the assumption that atrial and ventricular activity are independent. While it is certainly not a valid assumption during SR, it may be during AF as the coupling between the atrial and the ventricular activity is influenced by the complex properties of the AV node.

The observed signal is the $M \times N$ matrix $\mathbf{X}$ which consists of ECG recordings from M leads, each of N samples length. The number of sources K is often defined beforehand and needs, in order for the ICA to work, to be less or equal to the number of signals, i.e. $K \leq M$. The $K \times N$ source signal matrix $\mathbf{S}$ is then defined as the matrix which, when multiplied with an unknown $M \times K$ mixing matrix $\mathbf{A}$, produces the observed signal $\mathbf{X}$,

$$\mathbf{X} = \mathbf{AS}. \tag{3.3}$$

The objective of the ICA is to obtain an estimate of $\mathbf{S}$, denoted $\hat{\mathbf{S}}$, by finding an inverse to $\mathbf{A}$

$$\hat{\mathbf{S}} = \mathbf{WX}, \tag{3.4}$$

where $\mathbf{W}$ serves as an estimate of the inverse of $\mathbf{A}$. The matrix $\mathbf{W}$ is chosen to maximize the independence between the source signals in $\hat{\mathbf{S}}$, usually done by maximizing the non-Gaussianity of the sources, quantified by, for example, the absolute value of kurtosis, i.e. the fourth order moment of the source signal. This relates to one of the fundamental assumptions regarding ICA for signal separation, that the signals to be separated are of non-Gaussian character, which appears to be valid for both the ventricular and the atrial component of the ECG signal. The ventricular signal has a super-Gaussian distribution while the atrial signal, with all its values more evenly distributed within an interval, has a sub-Gaussian distribution.

The extracted atrial activity signal using ICA is not related to any specific lead but rather a global atrial signal. As such, it can not be directly applied to, e.g., estimate f-wave amplitude (Sec. 3.3.2). A challenge is to identify which of the row vector of $\hat{\mathbf{S}}$ that corresponds to the desired atrial signal [81]. Methods based on ICA require more leads than ABS methods but does not depend upon beat detection and may be able to handle changing QRST morphologiess.

3.1.3   Adaptive filtering

Another approach to QRST cancellation is the use of adaptive filtering. The general idea is to select one lead, preferably one with substantial atrial activity like V_1 or V_2, as target signal $x_t(n)$, and another lead with considerably less atrial activity, like I or V_6, as reference signal $x_r(n)$. The reference signal is filtered and subtracted from $x_t(n)$ to obtain the error signal $e(n)$, which constitutes an estimate of the atrial activity signal.

In its most simple form, a linear filter is used, with weights obtained using the least mean square (LMS) algorithm to minimize the expected value of $e^2(n)$. However, this LMS approach has not proven very successful, with large QRST-related residuals due to the slow convergence of the filter weights, and has therefore not received much attention in the literature [82]. Instead, nonlinear techniques using neural networks, e.g. recurrent neural networks [83] or echo state neural networks (ESN) [84], have been proposed. In the ESN method, $x_r(n)$ is expanded to the vector $\mathbf{x}_r(n)$ which includes its first two derivatives, $x_r'(n)$ and $x_r''(n)$,

$$\mathbf{x}_r(n) = \begin{bmatrix} x_r(n) \\ x_r'(n) \\ x_r''(n) \end{bmatrix} , \tag{3.5}$$

offering a more complete characterization of the reference signal. The convergence is considerably faster than the LMS algorithm, which is crucial due to the rapid changes in QRST morphologies. The ESN was found to outperform ABS methods and was therefore chosen as atrial activity extraction method in Papers II, III, and IV. However, the requirement of a reference lead makes the ESN and other adaptive filtering methods unusable on single-lead ECG recordings. Also, it is crucial that the atrial activity is negligible in the reference signal to preserve the extracted f-waves, which may otherwise be heavily attenuated.

3.2 Modeling of atrial activity

The f-waves extracted from ECG signals may not be sufficient, e.g., when the purpose of the study is to evaluate the f-wave extraction method itself [78, 85], or when detection of brief AF episodes, rarely encountered in annotated databases, is to be studied [86]. This need is catered for by the introduction of simulated f-waves, designed to replicate the appearance and behaviour of waves from actual recordings. Simulation also offer the advantage of being able to control f-wave properties, such as frequency and amplitude, in detail, thus enabling the evaluation of estimation procedures [87]. Models for creating complete synthetic ECG signals with ventricular activity have also been proposed [88, 89], and P-waves have been modeled using a linear combination of Hermite functions [90].

A widely used f-wave model was originally introduced in [78] and further developed in [84]. Referred to as the *f-wave sawtooth model*, it consists of a number of sinusoids modulated both in frequency and amplitude, and is capable of creating sawtooth-shaped f-waves. The sawtooth signal $x_s(n)$ is defined as

$$x_s(n) = \sum_{k=1}^{K} a_k(t) \sin\left(2\pi k f_0 n + k\frac{\Delta F}{F_m}\sin(2\pi F_m n)\right), \quad (3.6)$$

where f_0 defines the DAF, an important f-wave parameter discussed in further detail in Sec. 3.3.1. The number of included harmonics is denoted K and the variables ΔF and F_m define maximum frequency deviation, and the DAF modulation frequency, respectively. The amplitude of the k:th harmonic is defined by $a_k(n)$,

$$a_k(n) = \frac{2}{k\pi}\left(a + \Delta a \sin(2\pi F_a n)\right), \quad k = 1, \ldots, K, \quad (3.7)$$

where a is the mean f-wave amplitude while Δa and F_a define the maximum amplitude deviation, and the amplitude modulation frequency, respectively. To create a more challenging f-wave signal for extraction purposes, a stochastic component can be added. In [84], this was performed by adding colored noise consisting of frequencies close to f_0. An example of simulated f-waves from the f-wave sawtooth model is presented in Fig. 3.2.

While the purpose of the f-wave sawtooth model is to simulate f-waves, it may not perform well in the context of parameter estimation due to its relatively large number of variables. A simpler *harmonic f-wave model*, designed for estimation purposes, is introduced in Paper II. The model f-wave signal $x_h(n)$, now assumed to be complex-valued, is defined as

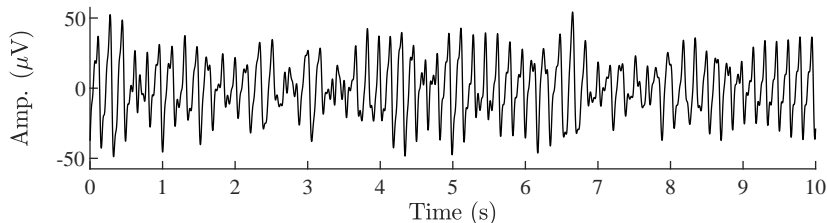$$x_h(n) = \sum_{k=1}^{K} A_k e^{j(2\pi k f_0 n + \phi_k)}, \quad (3.8)$$

Figure 3.2: Example of simulated f-waves from the f-wave sawtooth model, including the stochastic component proposed in [84].
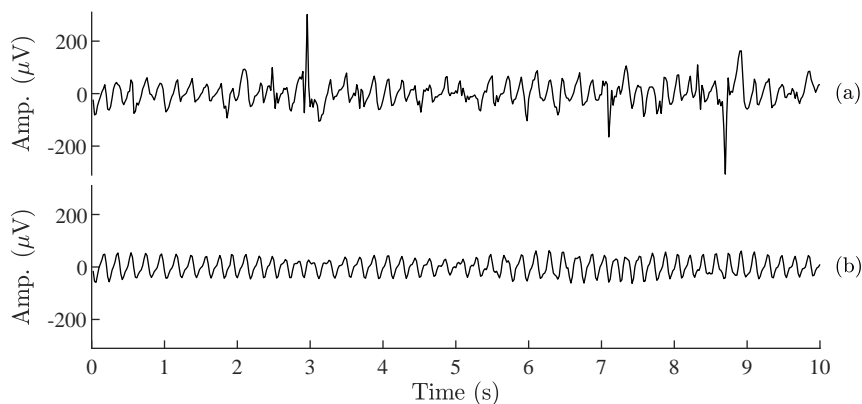
Figure 3.3: (a) Extracted f-waves $x(n)$ and (b) the corresponding model f-waves $x_h(n)$.

where the amplitude and phase of the k:th harmonic is defined by A_k and ϕ_k, respectively. An example of extracted f-waves $x(n)$ obtained using spatiotemporal QRST cancellation and the corresponding $x_h(n)$ is presented in Fig. 3.3. Originally used for DAF estimation, the harmonic f-wave model has also been used to estimate parameters related to amplitude and phase [91]. In [92], an similar approach, also using the sum of a sinusoid and its harmonics, was taken to reconstruct an f-wave signal from $f(n)$. Band-pass filters centred around the estimated DAF and its harmonics were applied to decompose $x(n)$ into narrowband components and the information obtained from each component was used to define the amplitude, frequency and phase of the sinusoid and its harmonics in the reconstructed signal. The phase information was used to quantify morphological properties.

3.3 Characterization of atrial activity

Once f-waves are extracted or simulated, the atrial activity can be characterized using various f-wave parameters. While atrial activity analysis based on f-waves lacks the spatial precision of invasive methods and has not yet found its way to clinical practice, it opens up new possibilities for diagnostics and monitoring due to its accessibility and potential long-term use.

Studies have linked f-wave parameters to the spontaneous termination of paroxysmal AF [93, 94, 95], AF type (paroxysmal/persistent) [96, 97], and the outcome of catheter ablation [98, 99, 100, 101, 102, 103, 104]. Other studies have used f-wave parameters to evaluate the effect of antiarrhythmic drugs [105, 106, 107].

Although f-wave parameters may be computed from any lead, V_1 is most frequently used when 12-lead recordings are available. This is due to its relative proximity to the right atrium, which provides f-waves of greater magnitude than other leads [108]. The extracted f-wave signal is denoted $x(n)$ in the following.

3.3.1 Dominant atrial frequency

The DAF f_0 constitutes one of the most widely used parameters characterizing f-waves. It is equivalent to the atrial fibrillatory rate used in some studies, and the inverse of dominant atrial cycle length (DACL), commonly used in clinical studies. Historically, the DACL was obtained by measuring the distance in time between atrial activations in invasive electrogram recordings from the left or right atrium [109, 110]. However, it has been shown that similar information is available non-invasively from the ECG by localizing the dominant spectral peak in the frequency spectrum of the f-waves [111]. An example of DAF estimation from the frequency spectrum is illustrated in Fig. 3.4. Another DAF estimation approach, which is based on the harmonic f-wave model in (3.8) and MLE, is introduced in Paper II.

Sample-by-sample DAF estimates $\hat{f}_0(n)$ can be provided using an adaptive line enhancer [112]. The narrowband signal $y(n)$ is obtained by bandpass filtering $x(n)$ around the previous DAF estimate $\hat{f}_0(n-1)$. The DAF estimate is then updated by minimizing the squared error of the one-step predictor on $y(n-1)$,

$$\hat{f}_0(n) = \arg\min_{f_0(n)} \left\| y(n) - e^{j2\pi f_0(n)} y(n-1) \right\|^2 . \qquad (3.9)$$

The frequency tracker can be extended to also include harmonic components. Several narrowband signals are then created, one centered around each harmonic, and frequency estimates from each signal are combined to provide a DAF estimate. The
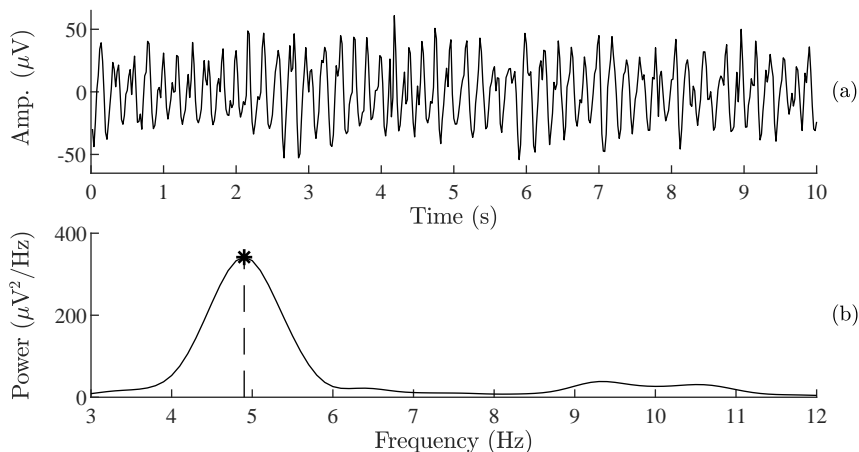
Figure 3.4: Example of (a) f-waves and (b) the corresponding power spectra obtained using Welch's method. The estimated DAF at 4.9 Hz is marked with a star.

DAF trend can also been post-processed using a hidden Markov model to remove outliers [113].

The DAF is expected to exist within a certain frequency band, and thus only spectral peaks within this band are of interest when determining the DAF. Many studies consider the range of the DAF to be 3–12 Hz, but other studies have suggested that the extremes are very rare and that the search may be limited to, e.g., 4–9 Hz [108]. In a study of paroxysmal AF patient, all DAF estimates were in the range 4–7 Hz [114].

3.3.2   Amplitude

Other than the DAF, the f-wave amplitude is the most widely used f-wave parameter and has a long history in clinical AF analysis [115, 116, 117]. Initially, the analysis was confined to manually classifying the f-waves as "coarse" or "fine" depending on whether the amplitude was found to be greater or less than 50 μV. The relationship between f-wave amplitude and specific clinical properties have been the subject of conflicting results, with some studies finding a correlation between, e.g., amplitude and left atrial size [118], while others do not [119]. It has been suggested that this could be due to interpatient variations in chest wall thickness [108].

One challenge with estimating the f-wave amplitude is the obvious sensitivity to QRS-related residuals, which, if present, may severely distort the estimate. One approach to f-wave amplitude estimation is therefore to exclude segments containing
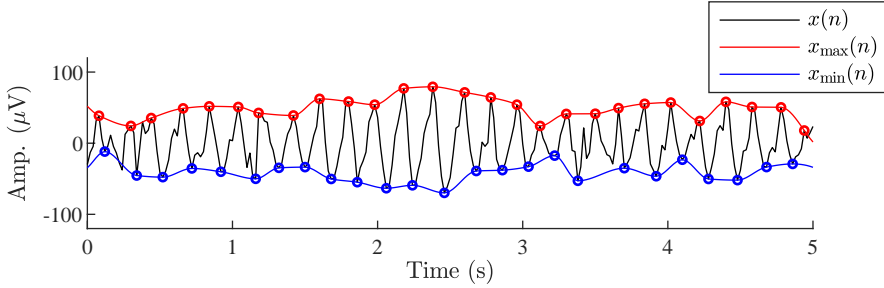
Figure 3.5: Example of amplitude estimation using envelope detection. The local maxima and minima are marked with circles.

QRS complexes and only use the remainder of the f-wave signal. The amplitude has been defined as the mean of four largest f-wave peaks in 10 s segment [120, 121]. Another option is to obtain an amplitude estimate $\hat{a}$ from N_x samples of $x(n)$ using envelope detection based on local extrema,

$$\hat{a} = \frac{1}{N_x} \sum_{n=0}^{N_x-1} |x_{\max}(n) - x_{\min}(n)| , \qquad (3.10)$$

where $x_{\max}(n)$ and $x_{\min}(n)$ are obtained using piecewise cubic Hermite interpolating polynomials on successsive local maxima and minima, respectively, of $x(n)$ [99]. An example of $x_{\max}(n)$ and $x_{\min}(n)$ is presented in Fig. 3.5.

An alternative f-wave magnitude measure is to compute the root-mean-square (RMS) of $x(n)$ [122]. The energy has also been computed from the main atrial wave, obtained by filtering $x(n)$ with a bandpass filter centered around the DAF [123].

3.3.3 Complexity and regularity

In addition to the DAF and f-wave amplitude, a large number of other parameters quantifying the complexity, morphology, and regularity of f-waves have been presented [124, 125, 126, 127, 128, 129]. This subsection does not intend to provide a complete overview of this extensive field, but rather present some metrics applied in the included papers.

The f-wave organization may be quantified in the spectral domain by the *spectral*

organization index S_{OI}, computed from the power spectral density of $x(n)$, $P_x(f)$,

$$S_{\mathrm{OI}} = \frac{\displaystyle\sum_{k=1}^{K} \int_{-\Delta f/2}^{\Delta f/2} P_x(f_k + f)\mathrm{d}f}{\displaystyle\int_{f_{\min}}^{f_{\max}} P_x(f)\mathrm{d}f}, \tag{3.11}$$

where f_k is the position of the k:th harmonic, K is the number of harmonics, and Δf is the spectral width [130]. The integration limits $f_{\min}$ and $f_{\max}$ have been set to 2.5 Hz and the beginning of the $(K + 1)$ harmonic peak, respectively [131].

Contrary to other f-wave parameters described in this thesis, the PCA-based *spatiotemporal variability* ϵ makes use of multiple ECG leads [104]. The f-wave signal is partitioned into four subsegments of equal length and one-dimensional principal subspaces are computed for each subsegment. The s:th subsegment of $x(n)$, denoted $x^{(s)}(n)$, is projected to the r:th subspace and the normalized mean square error $\epsilon(r, s)$ is computed,

$$\epsilon(r, s) = \frac{\displaystyle\sum_{n=1}^{N_x/4} \left(x^{(s)}(n) - \hat{x}^{(r,s)}(n) \right)^2}{\displaystyle\sum_{n=1}^{N_x/4} (x^{(s)}(n))^2} \quad r, s = 1, \dots, 4, \tag{3.12}$$

where $\hat{x}^{(r,s)}(n)$ denotes the projection and ϵ is obtained by averaging $\epsilon(r, s)$ over all possible s and r, $s \neq r$.

Paper IV introduces the *phase dispersion* γ, an f-wave parameter which describes the stability of the atrial waveform. The harmonic f-wave model in (3.8) is used to estimate the phase parameters $\hat{\phi}_1(n)$ and $\hat{\phi}_2(n)$, and γ is defined as

$$\gamma = \left| \frac{1}{N_x} \sum_{n=0}^{N_x-1} e^{j(\hat{\phi}_2(n) - 2\hat{\phi}_1(n))} \right|, \tag{3.13}$$

where $0 < \gamma \leq 1$. A stable f-wave morphology corresponds to a constant phase difference between the harmonics and $\gamma \approx 1$, while morphological variation lowers γ. The reproducibility of the DAF, f-wave amplitude, S_{OI}, ϵ and γ is the topic of Paper V.

3.3.4 Detection of atrial fibrillation using atrial information

The rhythm-based AF detectors described in Sec. 2.1.3 can perform very well, in particular when evaluated on a dataset consisting only of AF and SR. However, in many real applications, false AF detections frequently occur due to non-AF arrhythmias displaying rhythm patterns similar to those of AF. Including atrial information in the detector can improve its specificity, but adds extra levels of complexity; both in terms of computational demand, but also due to increased susceptibility to noise. Another benefit of including atrial information is the possibility to detect very brief episodes of AF, too short to manifest an irregular rhythm. A general scheme for an AF detector which may involve both rhythm-based analysis and atrial information is illustrated in Fig. 3.6.

The presence of P-waves have been determined by comparing the length and morphology of consecutive PR intervals, defined as the time between P-wave onset and QRS onset [132]. Extending a rhythm-based detector with these metrics improved its performance, in particular its specificity and positive predictive value.

In [133], a detector exclusively based on detection of P-wave absence was proposed. A beat detection algorithm is used to identify segments where P-waves are expected to appear and nine features related to P-wave presence are computed from each segment. The method was capable of detecting AF in as few as seven beats, using only one lead. However, the method was found to be ineffective in noisy environments.

Another approach, using *wavelet entropy*, was presented in [134]. Wavelet functions $\psi_{u,v}(n)$ are defined by scaling and translating a predefined mother wavelet $\psi(n)$,

$$\psi_{u,v}(n) = 2^{-\frac{u}{2}}\psi\left(2^{-u}n - v\right), \quad u = 1, \ldots, N_u, \quad v = 1, \ldots, N_v, \quad (3.14)$$

where N_u is the number of wavelet decomposition levels and N_v is the maximum translation. Wavelet coefficients $C(u, v)$ are computed from the correlations between the median of TQ intervals, $m_{\mathrm{TQ}}(n)$, and $\psi_{u,v}(n)$,

$$C(u, v) = \sum_{n=1}^{N_{\mathrm{TQ}}} m_{\mathrm{TQ}}(n)\psi_{u,v}(n), \quad (3.15)$$

where N_{TQ} is the length of $m_{\mathrm{TQ}}(n)$. The coefficients $C(u, v)$ are then used to compute the relative energies for each wavelet decomposition level E_u,

$$E_u = \frac{\sum_{v=1}^{N_v} C^2(u, v)}{\sum_{u=1}^{N_u} \sum_{v=1}^{N_v} C^2(u, v)}. \quad (3.16)$$

The wavelet entropy I_{W}, defined as the Shannon entropy of E_u, cf. (2.5), is used as the detection metric. Signals containing P-waves are associated with a significantly
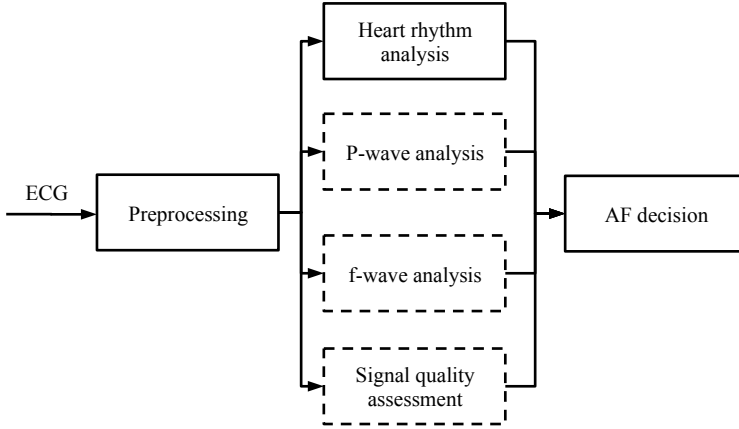
Figure 3.6: Schematic overview over an AF detection algorithm [86]. The prepro-
cessing step typically involves beat detection and, for some methods, atrial activity
extraction. Rhythm-based analysis constitutes the by far most common approach
to AF detection.

lower I_W than those containing f-waves. Limiting the analysis to TQ intervals re-
moves the need for atrial activity extraction, however, it also complicates analysis
during fast heart rates, where the TQ interval is shortened. Detection approaches
completely based on atrial information have displayed performance inferior to the
best-performing rhythm-based AF detectors [135]. Therefore, it is suggested that
rhythm-based analysis should be included.

An AF detector which combines rhythm-based analysis with atrial information
was presented in [86]. The absence of P-waves is quantified by $\mathcal{P}$, the mean squared
error between PR intervals. The value of $\mathcal{P}$ is expected to be close to zero when
P-waves are present because of their regularity compared to f-waves. Additionally,
the method also uses a measure of f-wave presence, $\mathcal{F}$, computed by the normalized
spectral concentration of $x(n)$,

$$\mathcal{F} = \frac{1}{E_x} \int_\Omega P_x(f)\mathrm{d}f, \tag{3.17}$$

where P_x is the power spectrum of $x(n)$ and E_x is the energy of $x(n)$. The in-
tegration interval Ω is centered around the dominant spectral peak (Note that this
makes $\mathcal{F}$ identical to S_{OI} for $K = 1$ in (3.11). The value of $\mathcal{P}$ and $\mathcal{F}$ are combined
with measures of rhythm irregularity and noise level (See Sec. 3.4) into the detection
output $\mathcal{O}$. In Fig. 3.7, the detection performance of $\mathcal{O}$ is demonstrated for the same
example which was subjected to rhythm-based AF detection in Fig. 2.3. The inclu-
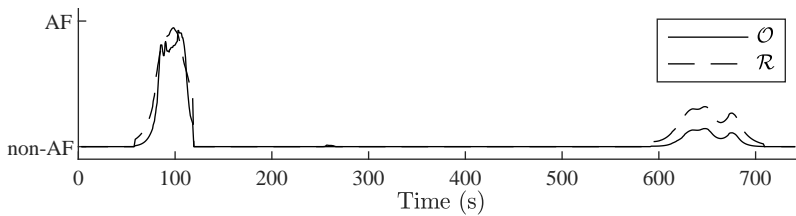
Figure 3.7: The output of the rhythm- and morphology-based AF detector $\mathcal{O}$ (solid line), and the rhythm-based AF detector $\mathcal{R}$ (dashed line). The example is the same as in Fig. 2.3.

sion of atrial information further attenuates the detection output during the non-AF arrhythmic episode, thereby reducing the risk of a false alarm.

Recent approaches to AF detection include machine learning methods such as the use of deep convolution neural networks, which uses the short-term Fourier transform or the stationary wavelet transform of the ECG signal, i.e. with both ventricular and atrial information, as input [136]. While the presented detection performance is very good, the method was evaluated on a random subset of AFDB and the results can therefore not be directly compared to those of other detectors [137]. In [138], the band-pass filtered ECG signal is subjected to a wavelet transform for extraction of AF detection features. The extracted features are subsequently used to classify the signal as AF, or non-AF, using a machine learning approach. The method performed well when comparing with methods dependent upon beat detection. However, the inability to detect short AF episodes was mentioned as a potential limitation.

3.4   Quality assessment of atrial activity

One aspect of atrial activity analysis, which has received remarkably little research attention, is that of signal quality assessment. The relatively low amplitude of P-waves and f-waves make them considerably more likely to be corrupted by noise, while, at the same time, the computed parameters may attempt to include detailed morphological information. One study showed that the sample entropy of the atrial activity signal increased with noise, which seriously impairs the discriminatory power of that parameter in noisy environments [95]. It is very likely that other f-wave parameters exhibit similar behaviour. While the methods described in Sec. 2.2 may perform very well for rhythm-based analysis, they are of little help when atrial activity is studied.

The AF detectors described in Sec. 3.3.4 rely on analysis of morphology and can therefore be very sensitive to noise. The wavelet entropy detector handles this issue by discarding individual TQ intervals where the wavelet entropy exceeds a predefined threshold prior to computing the median TQ interval $m_{\mathrm{TQ}}(n)$ [134], turning wavelet entropy to both a quality and a detection metric.

In [86], a noise level estimator was included in the AF detector. The noise parameter $\mathcal{N}$ is defined as

$$\mathcal{N} = R_x \frac{\int_{f_{n,0}}^{f_{n,1}} P_x(f) \log_2 P_x(f) \mathrm{d}f}{\int_{f_{a,0}}^{f_{a,1}} P_x(f) \log_2 P_x(f) \mathrm{d}f} \qquad (3.18)$$

where R_x is the RMS of $x(n)$. The parameters $f_{a,0}$ and $f_{a,1}$ define the frequency range expected to contain the f-waves while $f_{n,0}$ and $f_{n,1}$ define the frequency range of the noise. The parameter $\mathcal{N}$ was shown to be proportional to the noise level, while essentially independent of f-wave amplitude.

The inability of $\mathcal{N}$ to detect noise contained within the same frequency band as the f-waves is the main motivation for Paper II in this thesis, which introduces a novel f-wave SQI defined by the error between the harmonic f-wave model $x_h(n)$ in (3.8) and the extracted f-wave signal $x(n)$.

Chapter 4

Summary of the Included Papers

This chapter present summaries of the five included papers on ECG analysis of AF. Significant research contributions include a statistical approach to estimation of AV nodal properties (Paper I), a novel f-wave SQI (Paper II), a demonstration of the influence of f-wave signal quality in DAF estimation (Paper III), a study of ablation-induced changes in f-wave characteristics (Paper IV), and an investigation of the difference in reproducibility among f-wave parameters (Paper V).

The estimation approach in Paper I is shown to be more robust than that of a reference method and the f-wave SQI of Paper II is applied to select which signals to use in Papers III–V. In conclusion, the studies introduce novel methods while demonstrating the significance of robustness and quality assessment.

4.1   Paper I - A Statistical Atrioventricular Node Model Accounting for Pathway Switching During Atrial Fibrillation

This paper presents a novel statistical dual pathway AV node model which allows atrial impulses to switch between AV nodal pathways although the previous impulse was blocked.

A major drawback of the AV node model presented in [64, 65], referred to as the reference model in the following, was the substantial variation in parameters estimates, a property commonly associated with too many degrees of freedom. Reducing the number of model parameters is therefore assumed to decrease the variance and improve the reliability of the estimates. Similar to the models in [64, 65], atrial impulses are assumed to arrive at the AV node according to a Poisson process with an intensity related to the DAF. However, unlike the previous model, the ratio of conducted impulses through either pathway is not a model parameter but instead, equal probability for attempted conduction through either pathway is assumed. This reduces the number of model parameters subjected to MLE from five to four, with two parameters describing each pathway.

The ratio of all atrial impulses conducted through the slow pathway α, previously a model parameter, is now computed from the estimated parameters and used as a reliability metric. A small α implies a smaller share of the conducted impulses passing through the slow pathway, and, therefore, reduces the reliability of the two parameters defining the slow pathway. Conversely, a large α reduces the reliability of the two parameters defining the slow pathway. Individual α-thresholds are defined for each of the parameters and used to determine whether the estimate is included in further analysis.

The model is evaluated using RR interval histograms from the RATe control in Atrial Fibrillation (RATAF) database, involving 24-h recordings from 60 permanent AF patients [27]. The parameter reduction does not impair the modelling ability as similar results are obtained for both the present and the reference model, with a median fit of 86%. The model is still capable of modelling bimodal RR interval histograms, as illustrated in Fig. 4.1.

Comparison with the reference model reveals significantly less variation in three of the four parameters in the new model. In particular, the parameters describing the longest refractory period prolongation of each pathway are considerably more robust and may be included in further research.
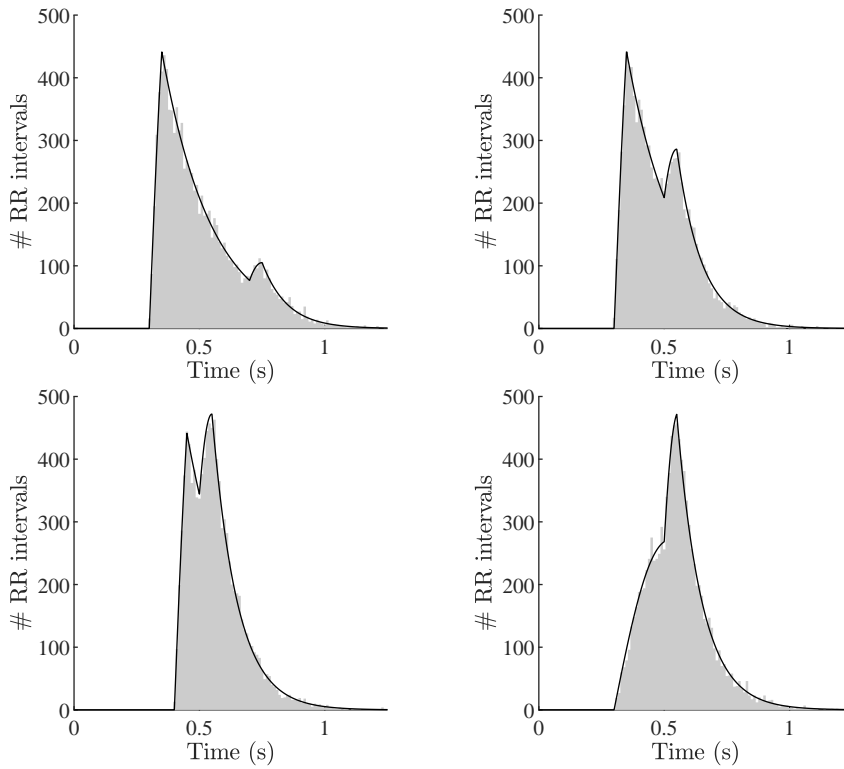
Figure 4.1: Examples of simulated RR interval histograms and probability density functions obtained with the AV node model from Paper I.

4.2   Paper II - Model-based Assessment of f-wave Signal Quality in Patients with Atrial Fibrillation

This paper introduces a novel f-wave SQI $\mathcal{S}$, and relates the value of $\mathcal{S}$ to the accuracy of DAF estimation, and how it can be indicative of f-wave presence and therefore used in AF detection. As described in Secs. 2.2 and 3.4, most of the SQIs found in the literature are designed to determine the reliability of beat detection and therefore not suitable for signal quality assessment of f-waves.

The computation of $\mathcal{S}$ consists of four steps and is based on the harmonic f-wave model $x_h(n)$ defined in (3.8). First, the DAF is estimated from $x(n)$ using MLE. Second, constrained estimation of the local DAF, allowing for minor deviations from the global estimate, is performed in overlapping subsegments of 0.5 s length. The complex phases of all subsegments are aligned and averaged to obtain a signal containing all frequency and phase information of $x_h(n)$. Third, the amplitudes of $x_h(n)$ are obtained minimizing the squared error between $x_h(n)$ and $x(n)$. Finally, $\mathcal{S}$ is obtained from the ratio of the RMS of $(x_h(n) - x(n))$ to the RMS of $x(n)$. The value of $\mathcal{S}$ allows for the identification and removal of noisy segments, as illustrated in Fig. 4.2.

The SQI is evaluated using simulated signals, 378 12-lead ECGs, and 1875 single-lead ECGs. Contrary to $\mathcal{N}$ defined in (3.18), $\mathcal{S}$ decreases with increasing noise levels even when the noise overlaps spectrally with f-waves. Moreover, the relationship between $\mathcal{S}$ and DAF estimation accuracy is established, with $\mathcal{S} > 0.3$ found to imply accurate estimation. The SQI $\mathcal{S}$ is substantially higher when computed from f-waves than from P-waves, suggesting that the SQI may be used in AF detection. This is investigated by replacing the f-wave presence measure $\mathcal{F}$ with $\mathcal{S}$ in the AF detector [86]. The detection performance improves with sensitivity increasing from 97.0% to 98.1% and the specificity increasing from 97.4% to 97.8%. It is concluded that $\mathcal{S}$ is well-suited to determine the quality of f-waves.
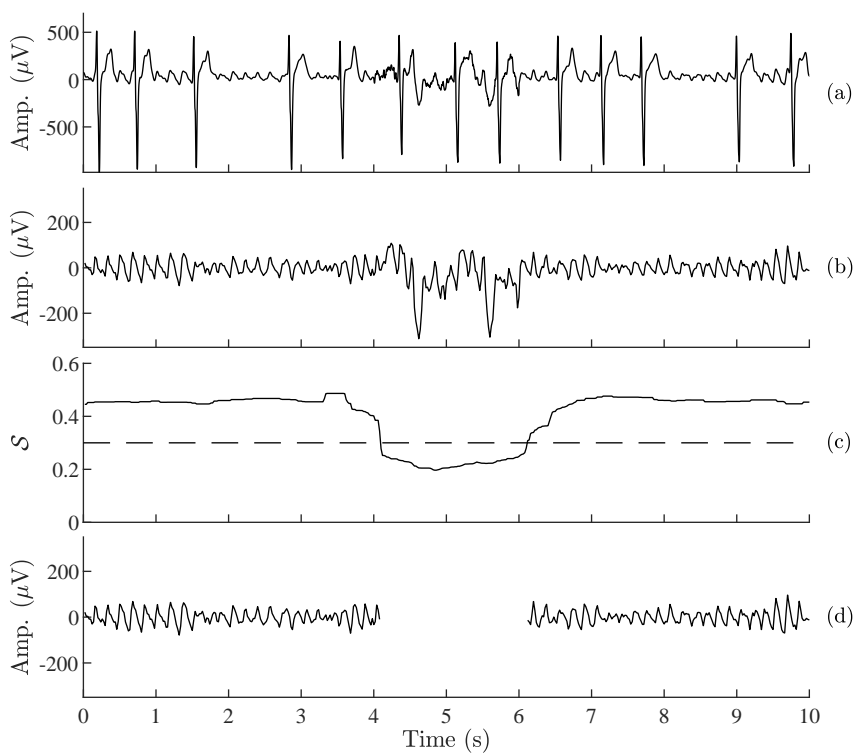
Figure 4.2: (a) ECG signal with noisy episode, (b) $x(n)$, (c) the f-wave SQI $\mathcal{S}$ with a threshold defining acceptable quality, and (d) $x(n)$, with the noisy episode removed according to $\mathcal{S}$.

4.3 Paper III - Atrial Fibrillation Frequency Tracking in Ambulatory ECG Signals: The Significance of Signal Quality Assessment

This paper revolves around tracking of the DAF in ambulatory 24h recordings. It includes 38 patients, all with permanent AF, and with ECG signals recorded from lead I, II, and V_1. The influence of signal quality and physical exercise is evaluated, as well as day- and night-time frequency variations.

The f-waves are obtained from the ECG using the echo state network extraction method on lead V_1 with lead I as the reference [84], and DAF estimates are obtained using the adaptive frequency tracker [112]. The f-wave SQI proposed in Paper II is slightly modified so that it is based on the output of the frequency tracker rather than the MLE of the DAF. Both the DAF and the SQI are computed from 5s segments, and segments not fulfilling the SQI-threshold of $\mathcal{S} \geq 0.2$ are excluded, see Fig. 4.3. Five patients are completely removed from the study after having more than 75% of their segments excluded, leaving 33 patients. Out of these 33 patients, 21 take part in physical activity during the recording, either by performing veloergometry (11 patients) or walking (10 patients).

Using the f-wave SQI to remove segments reduces the standard deviation of the DAF trend during both day- and night-time, from 0.46 ± 0.08 Hz to 0.36 ± 0.08 Hz, and from 0.38 ± 0.06 Hz to 0.30 ± 0.03 Hz, respectively. In both cases, the change is found to be statistically significant ($p \leq 0.001$ and $p \leq 0.01$, respectively). For the veloergometry subjects, a statistically significant ($p \leq 0.01$) decrease in SQI was observed during exercise, with the quality restored immediately afterwards. No significant SQI changes were observed during walking.

This study clearly demonstrates the importance of taking f-wave signal quality into consideration when tracking the DAF in ambulatory ECG signals. Visual inspection concluded that several recordings clearly were not feasible for this analysis, and in total, 40% of all segments were removed with the aid of the f-wave SQI.
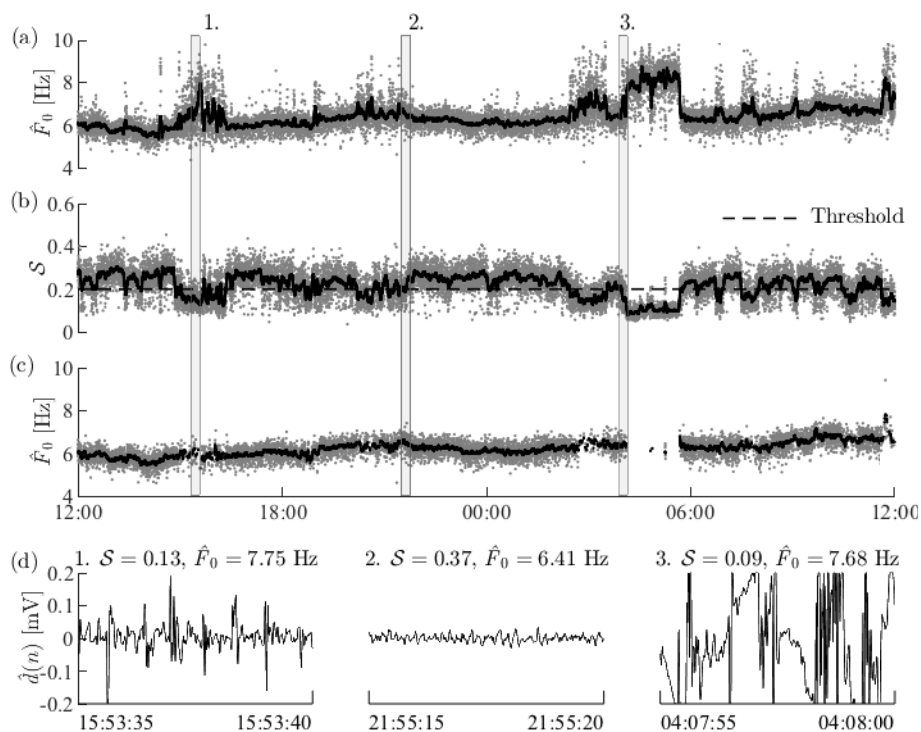
Figure 4.3: DAF tracking in a 24-h ambulatory ECG, with gray dots representing 5s estimates and the black solid line representing a smoothed series. (a) DAF series, (b) SQI series, (c) SQI-processed DAF series, and (d) three examples of f-waves: 1. f-waves corrupted by QRST residuals, 2. good quality f-waves, 3. f-waves corrupted by electrode movement artifacts.

4.4   Paper IV - Changes in f-wave Characteristics during Cryoballoon Catheter Ablation

This paper investigates the behaviour of three f-wave parameters computed in recordings obtained from AF patients undergoing pulmonary vein isolation using cryoballoon catheter ablation. The parameters are the DAF, the f-wave amplitude and the phase dispersion γ.

Numerous earlier studies have investigated the relationship between f-wave parameters and catheter ablation outcome. However, the results are inconsistent, with different studies suggesting that the same parameter is indicative of both success and failure. This could be due to different ablation protocols, or data sets not accounting for enough inter-patient variability. Another possible reason is extracardiac noise sources which may corrupt the parameter estimates. This study therefore includes the f-wave SQI from Paper II to eliminate low signal quality as a factor causing variation. Also, while most previous studies have limited the analysis to signals recorded prior to ablation, this study investigates ablation-induced changes. This is motivated by invasive studies which have observed changes in DACL during catheter ablation [139].

This study defines two datasets; dataset A, consisting of 12-lead ECG recordings from 77 AF patients (49/28 paroxysmal/persistent) obtained prior to the ablation, and dataset B, a subset of dataset A consisting of 31 AF patients (16/15 paroxysmal/persistent) where f-waves are available during the complete procedure. In both datasets, the f-wave SQI from Paper II is used to select which signal segment to analyze. Dataset A is used to assess the relationship between the parameters and clinical data. All parameters suggest clinical relevance as the DAF and γ were found to be related to AF type and the f-wave amplitude obtains significantly larger values in patients with increasing left atrial size.

The 31 patients in dataset B all underwent isolation of all four pulmonary veins and a total of five segments are thus obtained from each patient (prior ablation, in-between two isolations, and after ablation). The f-wave amplitude and γ did not exhibit any significant ablation-induced changes. However, the DAF displayed a significant decrease during the procedure ($p = 0.001$). This is illustrated in Fig. 4.4. No significant relation was found between the magnitude of the parameter change and the catheter ablation outcome.
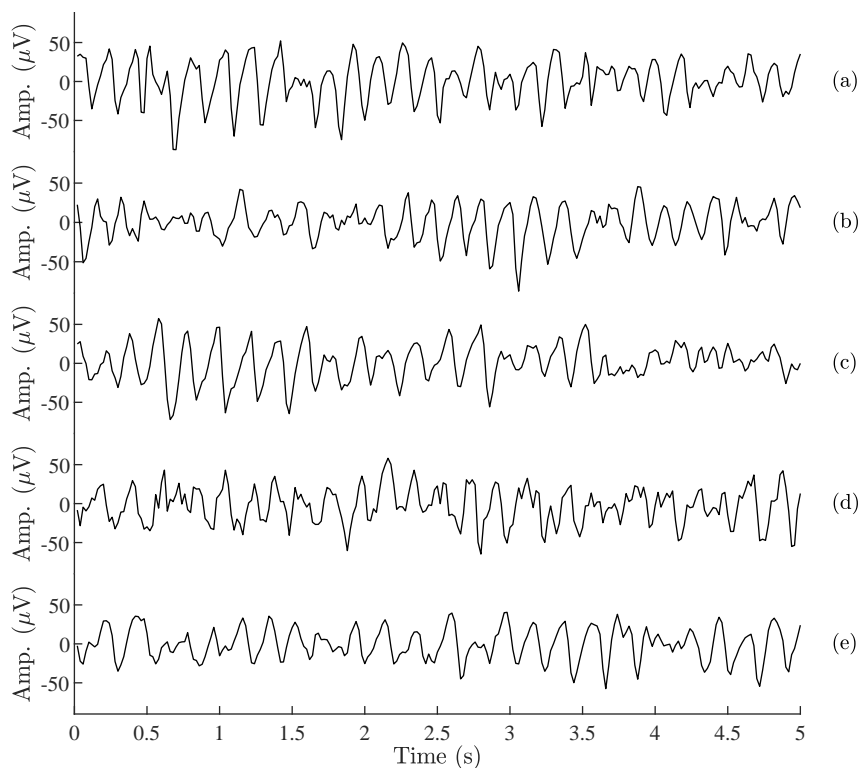
Figure 4.4: Example of a DAF decrease during ablation, with each subplot illustrating the f-waves after one additional pulmonary vein isolation. The DAF is: (a) 5.7 Hz, (b) 5.4 Hz, (c) 5.1 Hz, (d) 5.2 Hz and (e) 4.7 Hz.

4.5 Paper V - Reproducibility of parameters characterizing atrial fibrillatory waves

The paper investigates the reproducibility of five f-wave parameters by comparing their inter- and intrapatient variation. The considered parameters are the DAF, the f-wave amplitude, the phase dispersion γ, the spectral organization index S_{OI} and the spatiotemporal variability ϵ.

The dataset consists of a subset of the patients studied in Paper IV, consisting of 12-lead ECGs of 20 AF patients (11/9 paroxysmal/persistent). The recordings are of consistently high quality, assured using the f-wave SQI of Paper II. Spatiotemporal QRST cancellation is used to obtain the atrial activity signals and f-waves are present during the whole recording. The recording length varies between 20–200 min (92 ± 55 min, mean $\pm$ std).

The study is motivated by the considerable variation sometimes observed by repeated measurements of an f-wave parameter. By considering the variation of a 2 min window of a high-quality signal, changes caused by the treatment or noise are thought to be excluded as potential factors causing the variation, leaving only methodological reasons. The short-term variation is therefore quantified by the intrapatient variance σ^2 of a 2 min window while the interpatient variance τ^2 is computed from parameter estimates of different patients. The variance ratio R, defined as the ratio of σ^2 to τ^2, is used to quantify the reproducibility of each parameter, a larger R corresponding to better parameter stability and reproducibility.

The DAF is estimated using two different methods, namely the frequency tracker described in (3.9) and the MLE presented in Paper II, where the former results in a larger R ($R = 9.7$ and $R = 6.3$, respectively). The range of R-values of the DAF is presented in Fig. 4.5. The f-wave amplitude obtains $R = 21.0$ and $R = 25.4$ when estimated using the harmonic f-model in (3.8) and using envelope detection in (3.10), respectively. The remaining f-wave parameters all obtain considerably lower values of R, with $R = 2.4$, 2.4, and 2.7, for γ, S_{OI}, and ϵ, respectively. This study therefore demonstrates that there is a great difference in inter- and intrapatient variation among f-wave parameters, and that best reproducibility is to be found in the most established parameters of DAF and f-wave amplitude.
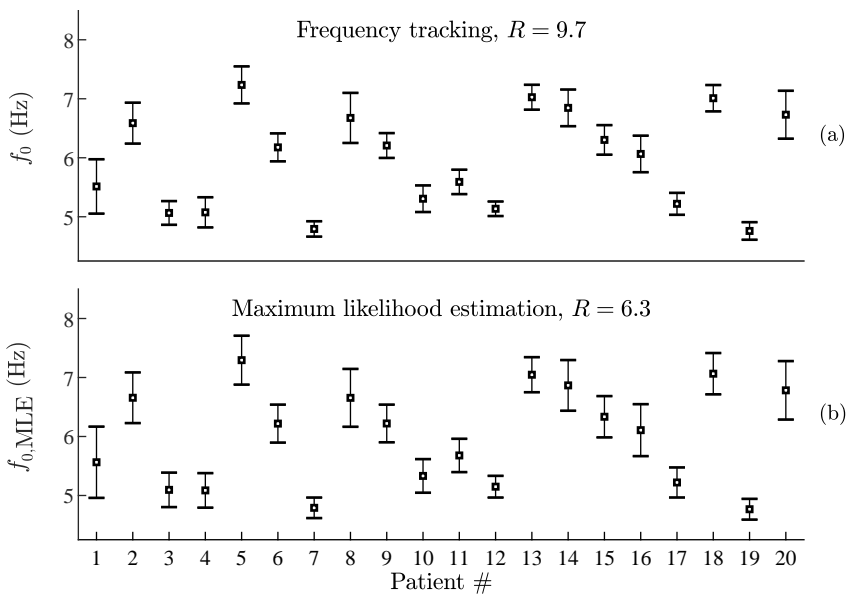
Figure 4.5: Comparison of DAF estimates obtained using (a) frequency tracking and (b) maximum likelihood estimation. The bars represent the standard deviation.

References

[1] L. Sörnmo and P. Laguna, *Bioelectrical signal processing in cardiac and neuro-logical applications*, vol. 8. Academic Press, 2005.

[2] P. Kirchhof, S. Benussi, D. Kotecha, A. Ahlsson, D. Atar, B. Casadei, M. Castella, H.-C. Diener, H. Heidbuchel, J. Hendriks, G. Hindricks, A. S. Manolis, J. Oldgren, B. A. Popescu, U. Schotten, B. Van Putte, and P. Vardas, "2016 ESC guidelines for the management of atrial fibrillation developed in collaboration with EACTS," *Eur. Heart J.*, vol. 37, no. 38, pp. 2893–2962, 2016.

[3] R. Nieuwlaat, A. Capucci, A. J. Camm, S. B. Olsson, D. Andresen, D. W. Davies, S. Cobbe, G. Breithardt, J.-Y. Le Heuzey, M. H. Prins, and S. Lúvy, "Atrial fibrillation management: a prospective survey in ESC member countries," *Eur. Heart J.*, vol. 26, no. 22, pp. 2422–2434, 2005.

[4] I. C. Van Gelder, H. F. Groenveld, H. J. Crijns, Y. S. Tuininga, J. G. Tijssen, A. M. Alings, H. L. Hillege, J. A. Bergsma-Kadijk, J. H. Cornel, O. Kamp, R. Tukkie, H. A. Bosker, D. J. Van Veldhuisen, and M. P. Van den Berg, "Lenient versus strict rate control in patients with atrial fibrillation," *N. Engl. J. Med.*, vol. 362, no. 15, pp. 1363–1373, 2010.

[5] M. Haissaguerre, P. Jaïs, D. C. Shah, A. Takahashi, M. Hocini, G. Quiniou, S. Garrigue, A. Le Mouroux, P. Le Métayer, and J. Clémenty, "Spontaneous initiation of atrial fibrillation by ectopic beats originating in the pulmonary veins," *N. Engl. J. Med.*, vol. 339, no. 10, pp. 659–666, 1998.

[6] A. V. Sarabanda, T. J. Bunch, S. B. Johnson, S. Mahapatra, M. A. Milton, L. R. Leite, G. K. Bruce, and D. L. Packer, "Efficacy and safety of circumferential

pulmonary vein isolation using a novel cryothermal balloon ablation system," *J. Am. Coll. Cardiol.*, vol. 46, no. 10, pp. 1902–1912, 2005.

[7] A. Luik, A. Radzewitz, M. Kieser, M. Walter, P. Bramlage, P. Hörmann, K. Schmidt, N. Horn, M. Brinkmeier-Theofanopoulou, K. Kunzmann, T. Riexinger, G. Schymik, M. Merkel, and C. Schmitt, "Cryoballoon versus open irrigated radiofrequency ablation in patients with paroxysmal atrial fibrillation: the prospective, randomised, controlled, non-inferiority FreezeAF study," *Circulation*, pp. 1311–1319, 2015.

[8] K.-H. Kuck, J. Brugada, A. Fürnkranz, A. Metzner, F. Ouyang, K. J. Chun, A. Elvan, T. Arentz, K. Bestehorn, S. J. Pocock, J.-P. Albenque, and C. Tondo, "Cryoballoon or radiofrequency ablation for paroxysmal atrial fibrillation," *N. Engl. J. Med.*, vol. 374, no. 23, pp. 2235–2245, 2016.

[9] H. Oral, B. P. Knight, H. Tada, M. Ozaydın, A. Chugh, S. Hassan, C. Scharf, S. W. Lai, R. Greenstein, F. Pelosi Jr., A. Strickberger, and F. Morady, "Pulmonary vein isolation for paroxysmal and persistent atrial fibrillation," *Circulation*, vol. 105, no. 9, pp. 1077–1081, 2002.

[10] A. G. Brooks, M. K. Stiles, J. Laborderie, D. H. Lau, P. Kuklik, N. J. Shipp, L.-F. Hsu, and P. Sanders, "Outcomes of long-standing persistent atrial fibrillation ablation: a systematic review," *Heart Rhythm*, vol. 7, no. 6, pp. 835–846, 2010.

[11] F. Ouyang, R. Tilz, J. Chun, B. Schmidt, E. Wissner, T. Zerm, K. Neven, B. Köktürk, M. Konstantinidou, A. Metzner, A. Fuernkranz, and K.-H. Kuck, "Long-term results of catheter ablation in paroxysmal atrial fibrillation," *Circulation*, vol. 122, no. 23, pp. 2368–2377, 2010.

[12] R. Cappato, H. Calkins, S.-A. Chen, W. Davies, Y. Iesaka, J. Kalman, Y.-H. Kim, G. Klein, A. Natale, D. Packer, A. Skanes, F. Ambrogi, and E. Biganzoli, "Updated worldwide survey on the methods, efficacy and safety of catheter ablation for human atrial fibrillation," *Circ. Arrhythm. Electrophysiol.*, vol. 3, no. 1, pp. 32–38, 2010.

[13] Z. Ihara, A. van Oosterom, V. Jacquemet, and R. Hoekema, "Adaptation of the standard 12-lead electrocardiogram system dedicated to the analysis of atrial fibrillation," *J. Electrocardiol.*, vol. 40, no. 1, pp. 68–e1, 2007.

[14] A. Kennedy, D. D. Finlay, D. Guldenring, R. R. Bond, and J. McLaughlin, "Detecting the elusive P-wave: a new ECG lead to improve the recording of atrial activity," *IEEE Trans. Biomed. Eng.*, vol. 63, no. 2, pp. 243–249, 2016.

[15] A. Petrėnas, V. Marozas, G. Jaruševičius, and L. Sörnmo, "A modified Lewis ECG lead system for ambulatory monitoring of atrial arrhythmias," *J. Electrocardiol.*, vol. 48, no. 2, pp. 157–163, 2015.

[16] E. Svennberg, J. Engdahl, F. Al-Khalili, L. Friberg, V. Frykman, and M. Rosenqvist, "Mass screening for untreated atrial fibrillation: the STROKESTOP study," *Circulation*, pp. 2176–2184, 2015.

[17] M. M. Baig, H. Gholamhosseini, and M. J. Connolly, "A comprehensive survey of wearable and wireless ECG monitoring systems for older adults," *Med. Biol. Eng. Comput.*, vol. 51, no. 5, pp. 485–495, 2013.

[18] S. S. Lobodzinski, "ECG patch monitors for assessment of cardiac rhythm abnormalities," *Prog. Cardiovasc. Dis.*, vol. 56, no. 2, pp. 224–229, 2013.

[19] J. Hayano, F. Yamasaki, S. Sakata, A. Okada, S. Mukai, and T. Fujinami, "Spectral characteristics of ventricular response to atrial fibrillation," *Am. J. Physiol.*, vol. 273, no. 6, pp. H2811–H2816, 1997.

[20] K. M. Stein, J. Walden, N. Lippman, and B. B. Lerman, "Ventricular response in atrial fibrillation: random or deterministic?," *Am. J. Physiol.*, vol. 277, no. 2, pp. H452–H458, 1999.

[21] J. Billette, R. A. Nadeau, and F. Roberge, "Relation between the minimum RR interval during atrial fibrillation and the functional refractory period of the AV junction," *Cardiovasc. Res.*, vol. 8, no. 3, pp. 347–351, 1974.

[22] V. D. Corino, S. R. Ulimoen, S. Enger, L. T. Mainardi, A. Tveit, and P. G. Platonov, "Rate-control drugs affect variability and irregularity measures of RR intervals in patients with permanent atrial fibrillation," *J. Cardiovasc. Electrophysiol.*, vol. 26, no. 2, pp. 137–141, 2015.

[23] S. Rokas, S. Gaitanidou, S. Chatzidou, C. Pamboucas, D. Achtipis, and S. Stamatelopoulos, "Atrioventricular node modification in patients with chronic atrial fibrillation role of morphology of RR interval variation," *Circulation*, vol. 103, no. 24, pp. 2942–2948, 2001.

[24] X. H. Guo, M. M. Gallagher, J. M. Bland, and A. J. Camm, "A distinctly bimodal distribution pattern in the RR interval histogram predicts early recurrence of atrial fibrillation after electrical cardioversion," *Int. J. Cardiol.*, vol. 145, no. 2, pp. 244–245, 2010.

[25] J. Tebbenjohanns, B. Schumacher, T. Korte, M. Niehaus, and D. Pfeiffer, "Bimodal RR interval distribution in chronic atrial fibrillation," *J. Cardiovasc. Electrophysiol.*, vol. 11, no. 5, pp. 497–503, 2000.

[26] R. Bousseljot, D. Kreiseler, and A. Schnabel, "Nutzung der EKG-signaldatenbank CARDIODAT der PTB über das internet," *Biomedizinische Technik*, vol. 40, no. 1, p. 317, 1995.

[27] S. R. Ulimoen, S. Enger, J. Carlson, P. G. Platonov, A. H. Pripp, M. Abdelnoor, H. Arnesen, K. Gjesdal, and A. Tveit, "Comparison of four single-drug regimens on ventricular rate and arrhythmia-related symptoms in patients with permanent atrial fibrillation," *Am. J. Cardiol.*, vol. 111, no. 2, pp. 225–230, 2013.

[28] A. Kennedy, D. D. Finlay, D. Guldenring, R. R. Bond, K. Moran, and J. McLaughlin, "Automated detection of atrial fibrillation using RR intervals and multivariate-based classification," *J. Electrocardiol.*, vol. 49, no. 6, pp. 871–876, 2016.

[29] J. S. Richman and J. R. Moorman, "Physiological time-series analysis using approximate entropy and sample entropy," *Am. J. Physiol.*, vol. 278, no. 6, pp. H2039–H2049, 2000.

[30] V. Tuzcu, S. Nas, T. Börklü, and A. Ugur, "Decrease in the heart rate complexity prior to the onset of atrial fibrillation," *Europace*, vol. 8, no. 6, pp. 398–402, 2006.

[31] A. Yamada, J. Hayano, S. Sakata, A. Okada, S. Mukai, N. Ohte, and G. Kimura, "Reduced ventricular response irregularity is associated with increased mortality in patients with chronic atrial fibrillation," *Circulation*, vol. 102, no. 3, pp. 300–306, 2000.

[32] I. Cygankiewicz, V. Corino, R. Vazquez, A. Bayes-Genis, L. Mainardi, W. Zareba, A. B. de Luna, and P. G. Platonov, "Reduced irregularity of ventricular response during atrial fibrillation and long-term outcome in patients with heart failure," *Am. J. Cardiol.*, vol. 116, no. 7, pp. 1071–1075, 2015.

[33] V. D. Corino, F. Holmqvist, L. T. Mainardi, and P. G. Platonov, "Beta-blockade and A1-adenosine receptor agonist effects on atrial fibrillatory rate and atrioventricular conduction in patients with atrial fibrillation," *Europace*, vol. 16, no. 4, pp. 587–594, 2013.

[34] V. D. Corino, I. Cygankiewicz, L. T. Mainardi, M. Stridh, R. Vasquez, A. Bayes de Luna, F. Holmqvist, W. Zareba, and P. G. Platonov, "Association between atrial fibrillatory rate and heart rate variability in patients with atrial fibrillation and congestive heart failure," *Ann. Noninv. Electrocardiol.*, vol. 18, no. 1, pp. 41–50, 2013.

[35] A. Petrėnas, V. Marozas, and L. Sörnmo, "Low-complexity detection of atrial fibrillation in continuous long-term monitoring," *Comp. Biol. Med.*, vol. 65, pp. 184–191, 2015.

[36] S. Dash, K. Chon, S. Lu, and E. Raeder, "Automatic real time detection of atrial fibrillation," *Ann. Biomed. Eng.*, vol. 37, no. 9, pp. 1701–1709, 2009.

[37] K. Tateno and L. Glass, "Automatic detection of atrial fibrillation using the coefficient of variation and density histograms of RR and δRR intervals," *Med. Biol. Eng. Comput.*, vol. 39, no. 6, pp. 664–671, 2001.

[38] X. Zhou, H. Ding, W. Wu, and Y. Zhang, "A real-time atrial fibrillation detection algorithm based on the instantaneous state of heart rate," *PloS one*, vol. 10, no. 9, pp. 1–16, 2015.

[39] D. E. Lake and J. R. Moorman, "Accurate estimation of entropy in very short physiological time series: the problem of atrial fibrillation detection in implanted ventricular devices," *Am. J. Physiol. Heart Circ. Physiol.*, vol. 300, pp. H319–H325, 2011.

[40] C. Liu, J. Oster, E. Reinertsen, Q. Li, L. Zhao, S. Nemati, and G. D. Clifford, "A comparison of entropy approaches for AF discrimination," *Physiol. Meas.*, 2018.

[41] C. Huang, S. Ye, H. Chen, D. Li, F. He, and Y. Tu, "A novel method for detection of the transition between atrial fibrillation and sinus rhythm," *IEEE Trans. Biomed. Eng.*, vol. 58, no. 4, pp. 1113–1119, 2011.

[42] J. Lian, L. Wang, and D. Muessig, "A simple method to detect atrial fibrillation using rr intervals," *Am. J. Cardiol.*, vol. 107, no. 10, pp. 1494–1497, 2011.

[43] J. Lee, Y. Nam, D. D. McManus, and K. H. Chon, "Time-varying coherence function for atrial fibrillation detection.," *IEEE Trans. Biomed. Eng.*, vol. 60, no. 10, pp. 2783–2793, 2013.

[44] J. Oster and G. D. Clifford, "Impact of the presence of noise on RR interval-based atrial fibrillation detection," *J. Electrocardiol.*, vol. 48, no. 6, pp. 947–951, 2015.

[45] G. B. Moody and R. G. Mark, "The impact of the MIT-BIH arrhythmia database," *IEEE Eng. Med. Biol. Mag.*, vol. 20, no. 3, pp. 45–50, 2001.

[46] A. L. Goldberger, L. A. Amaral, L. Glass, J. M. Hausdorff, P. C. Ivanov, R. G. Mark, J. E. Mietus, G. B. Moody, C.-K. Peng, and H. E. Stanley, "Physiobank, physiotoolkit, and physionet components of a new research resource for complex physiologic signals," *Circulation*, vol. 101, no. 23, pp. e215–e220, 2000.

[47] K. T. Sweeney, T. E. Ward, and S. F. McLoone, "Artifact removal in physiological signals–practices and possibilities," *IEEE Trans. Inf. Technol. Biomed.*, vol. 16, no. 3, pp. 488–500, 2012.

[48] M.-C. Chambrin, "Alarms in the intensive care unit: how can the number of false alarms be reduced?," *Crit Care.*, vol. 5, no. 4, p. 1, 2001.

[49] S. T. Lawless, "Crying wolf: false alarms in a pediatric intensive care unit.," *Crit. Care Med.*, vol. 22, no. 6, pp. 981–985, 1994.

[50] C. L. Tsien and J. C. Fackler, "Poor prognosis for existing monitors in the intensive care unit," *Crit. Care Med.*, vol. 25, no. 4, pp. 614–619, 1997.

[51] M.-C. Chambrin, P. Ravaux, D. Calvelo-Aros, A. Jaborska, C. Chopin, and B. Boniface, "Multicentric study of monitoring alarms in the adult intensive care unit (ICU): a descriptive analysis," *Int. Care Med.*, vol. 25, no. 12, pp. 1360–1366, 1999.

[52] D. P. Tobón V., T. H. Falk, and M. Maier, "MS-QI: a modulation spectrum-based ECG quality index for telehealth applications," *IEEE Trans. Biomed. Eng.*, vol. 63, no. 8, pp. 1613–1622, 2016.

[53] J. Allen and A. Murray, "Assessing ECG signal quality on a coronary care unit," *Physiol. Meas.*, vol. 17, no. 4, p. 249, 1996.

[54] G. Clifford, J. Behar, Q. Li, and I. Rezek, "Signal quality indices and data fusion for determining clinical acceptability of electrocardiograms," *Physiol. Meas.*, vol. 33, no. 9, p. 1419, 2012.

[55] J. Behar, J. Oster, Q. Li, and G. D. Clifford, "ECG signal quality during arrhythmia and its application to false alarm reduction," *IEEE Trans. Biomed. Eng.*, vol. 60, no. 6, pp. 1660–1666, 2013.

[56] Q. Li, C. Rajagopalan, and G. D. Clifford, "A machine learning approach to multi-level ECG signal quality classification," *Comput. Methods Programs Biomed.*, vol. 117, no. 3, pp. 435–447, 2014.

[57] C. Orphanidou, T. Bonnici, P. Charlton, D. Clifton, D. Vallance, and L. Tarassenko, "Signal-quality indices for the electrocardiogram and photo-plethysmogram: derivation and applications to wireless monitoring," *IEEE J. Biomed. Health Inf.*, vol. 19, no. 3, pp. 832–838, 2015.

[58] M. Abdelazez, P. X. Quesnel, A. D. Chan, and H. Yang, "Signal quality analysis of ambulatory electrocardiograms to gate false myocardial ischemia alarms," *IEEE Trans. Biomed. Eng.*, vol. 64, no. 6, pp. 1318–1325, 2017.

[59] N. Gambarotta, F. Aletti, G. Baselli, and M. Ferrario, "A review of methods for the signal quality assessment to improve reliability of heart rate and blood pressures derived parameters," *Med. Biol. Eng. & Comput.*, vol. 54, no. 7, pp. 1025–1035, 2016.

[60] U. Satija, B. Ramkumar, and M. S. Manikandan, "A review of signal processing techniques for electrocardiogram signal quality assessment," *IEEE Rev. Biomed. Eng.*, 2018.

[61] R. J. Cohen, R. D. Berger, and T. E. Dushane, "A quantitative model for the ventricular response during atrial fibrillation," *IEEE Trans. Biomed. Eng.*, no. 12, pp. 769–781, 1983.

[62] J. Lian, D. Mussig, and V. Lang, "Computer modeling of ventricular rhythm during atrial fibrillation and ventricular pacing," *IEEE Trans. Biomed. Eng.*, vol. 53, no. 8, pp. 1512–1520, 2006.

[63] J. Lian and D. Müssig, "Heart rhythm and cardiac pacing: an integrated dual-chamber heart and pacer model," *Ann. Biomed. Eng.*, vol. 37, no. 1, pp. 64–81, 2009.

[64] V. D. Corino, F. Sandberg, L. T. Mainardi, and L. Sornmo, "An atrioventricular node model for analysis of the ventricular response during atrial fibrillation," *IEEE Trans. Biomed. Eng.*, vol. 58, no. 12, pp. 3386–3395, 2011.

[65] V. D. Corino, F. Sandberg, F. Lombardi, L. T. Mainardi, and L. Sörnmo, "Atrioventricular nodal function during atrial fibrillation: Model building and robust estimation," *Biomed. Signal Process. Control*, vol. 8, no. 6, pp. 1017–1025, 2013.

[66] A. Rashidi and I. Khodarahmi, "Nonlinear modeling of the atrioventricular node physiology in atrial fibrillation," *J. Theor. Biol.*, vol. 232, no. 4, pp. 545–549, 2005.

[67] A. M. Climent, F. Atienza, J. Millet, and M. S. Guillem, "Generation of realistic atrial to atrial interval series during atrial fibrillation," *Med. Biol. Eng. Comput.*, vol. 49, no. 11, pp. 1261–1268, 2011.

[68] P. Jørgensen, C. Schäfer, P. G. Guerra, M. Talajic, S. Nattel, and L. Glass, "A mathematical model of human atrioventricular nodal function incorporating concealed conduction," *Bull. Math. Biol.*, vol. 64, no. 6, pp. 1083–1099, 2002.

[69] M. Wallman and F. Sandberg, "Characterisation of human AV-nodal properties using a network model," *Med. Biol. Eng. Comput.*, vol. 56, no. 2, pp. 247–259, 2018.

[70] S. Inada, J. Hancox, H. Zhang, and M. Boyett, "One-dimensional mathematical model of the atrioventricular node including atrio-nodal, nodal, and nodal-his cells," *Biophys. J.*, vol. 97, no. 8, pp. 2117–2127, 2009.

[71] V. D. A. Corino, F. Sandberg, P. G. Platonov, L. T. Mainardi, S. R. Ulimoen, S. Enger, A. Tveit, and L. Sörnmo, "Non-invasive evaluation of the effect of metoprolol on the atrioventricular node during permanent atrial fibrillation," *Europace*, vol. 16, no. Suppl 4, pp. iv129–iv134, 2014.

[72] V. D. Corino, F. Sandberg, L. T. Mainardi, P. G. Platonov, and L. Sörnmo, "Noninvasive assessment of atrioventricular nodal function: Effect of rate-control drugs during atrial fibrillation," *Ann. Noninv. Electrocardiol.*, vol. 20, no. 6, pp. 534–541, 2015.

[73] F. Sandberg, V. D. Corino, L. T. Mainardi, S. R. Ulimoen, S. Enger, A. Tveit, P. G. Platonov, and L. Sörnmo, "Non-invasive assessment of the effect of beta blockers and calcium channel blockers on the AV node during permanent atrial fibrillation," *J. Electrocardiol.*, vol. 48, no. 5, pp. 861–866, 2015.

[74] V. D. Corino, F. Sandberg, L. T. Mainardi, P. G. Platonov, and L. Sörnmo, "Noninvasive characterization of atrioventricular conduction in patients with atrial fibrillation," *J. Electrocardiol.*, vol. 48, no. 6, pp. 938–942, 2015.

[75] M. Henriksson, V. Corino, L. Sörnmo, and F. Sandberg, "A statistical atrioventricular node model accounting for pathway switching during atrial fibrillation," *IEEE Trans. Biomed. Eng.*, vol. 63, no. 9, pp. 1842–1849, 2016.

[76] Q. Xi, A. V. Sahakian, and S. Swiryn, "The effect of QRS cancellation on atrial fibrillatory wave signal characteristics in the surface electrocardiogram," *J. Electrocardiol.*, vol. 36, no. 3, pp. 243–249, 2003.

[77] P. Langley, J. J. Rieta, M. Stridh, J. Millet, L. Sornmo, and A. Murray, "Comparison of atrial signal extraction algorithms in 12-lead ECGs with atrial fibrillation," *IEEE Trans. Biomed. Eng.*, vol. 53, no. 2, pp. 343–346, 2006.

[78] M. Stridh and L. Sörnmo, "Spatiotemporal QRST cancellation techniques for analysis of atrial fibrillation," *IEEE Trans. Biomed. Eng.*, vol. 48, no. 1, pp. 105–111, 2001.

[79] A. Martínez, R. Alcaraz, and J. J. Rieta, "Ventricular activity morphological characterization: Ectopic beats removal in long term atrial fibrillation recordings," *Comput. Methods Programs Biomed.*, vol. 109, no. 3, pp. 283–292, 2013.

[80] J. J. Rieta, F. Castells, C. Sánchez, V. Zarzoso, and J. Millet, "Atrial activity extraction for atrial fibrillation analysis using blind source separation," *IEEE Trans. Biomed. Eng.*, vol. 51, no. 7, pp. 1176–1186, 2004.

[81] F. Castells, J. J. Rieta, J. Millet, and V. Zarzoso, "Spatiotemporal blind source separation approach to atrial activity estimation in atrial tachyarrhythmias," *IEEE Trans. Biomed. Eng.*, vol. 52, no. 2, pp. 258–267, 2005.

[82] L. Sörnmo, A. Petrėnas, P. Laguna, and V. Marozas, "Extraction of f waves," in *Atrial Fibrillation from an Engineering Perspective*, pp. 137–220, Springer, 2018.

[83] C. Vásquez, A. Hernandez, F. Mora, G. Carrault, and G. Passariello, "Atrial activity enhancement by wiener filtering using an artificial neural network," *IEEE Trans. Biomed. Eng.*, vol. 48, no. 8, pp. 940–944, 2001.

[84] A. Petrėnas, V. Marozas, L. Sörnmo, and A. Lukoševičius, "An echo state neural network for QRST cancellation during atrial fibrillation," *IEEE Trans. Biomed. Eng.*, vol. 59, no. 10, pp. 2950–2957, 2012.

[85] H. Dai, S. Jiang, and Y. Li, "Atrial activity extraction from single lead ECG recordings: Evaluation of two novel methods," *Comput. Biol. Med.*, vol. 43, no. 3, pp. 176–183, 2013.

[86] A. Petrėnas, L. Sörnmo, A. Lukoševičius, and V. Marozas, "Detection of occult paroxysmal atrial fibrillation," *Med. Biol. Eng. Comput.*, vol. 53, no. 4, pp. 287–297, 2015.

[87] M. Henriksson, A. Petrėnas, V. Marozas, F. Sandberg, and L. Sörnmo, "Model-based assessment of f-wave signal quality in patients with atrial fibrillation," *IEEE Trans. Biomed. Eng.*, vol. 65, no. 11, pp. 2600–2611, 2018.

[88] P. E. McSharry, G. D. Clifford, L. Tarassenko, and L. A. Smith, "A dynamical model for generating synthetic electrocardiogram signals," *IEEE Trans. Biomed. Eng.*, vol. 50, no. 3, pp. 289–294, 2003.

[89] A. Petrenas, V. Marozas, A. Sološenko, R. Kubilius, J. Skibarkiene, J. Oster, and L. Sörnmo, "Electrocardiogram modeling during paroxysmal atrial fibrillation: application to the detection of brief episodes," *Physiol. Meas.*, vol. 38, no. 11, pp. 2058–2080, 2017.

[90] L. Sörnmo, P. O. Börjesson, M.-E. Nygårds, and O. Pahlm, "A method for evaluation of QRS shape features using a mathematical model for the ECG," *IEEE Trans. Biomed. Eng.*, vol. 28, no. 10, pp. 713–717, 1981.

[91] M. Henriksson, A. García-Alberola, R. Goya, A. Vadillo, F.-M. Melgarejo-Meseguer, F. Sandberg, and L. Sörnmo, "Changes in f-wave characteristics during cryoballoon catheter ablation," *Physiol. Meas.*, vol. 39, no. 10, p. 105001, 2018.

[92] M. Stridh, D. Husser, A. Bollmann, and L. Sörnmo, "Waveform characterization of atrial fibrillation using phase information," *IEEE Trans. Biomed. Eng.*, vol. 56, no. 4, pp. 1081–1089, 2009.

[93] F. Nilsson, M. Stridh, A. Bollmann, and L. Sörnmo, "Predicting spontaneous termination of atrial fibrillation using the surface ECG," *Med. Eng. Phys.*, vol. 28, no. 8, pp. 802–808, 2006.

[94] S. Petrutiu, A. V. Sahakian, and S. Swiryn, "Abrupt changes in fibrillatory wave characteristics at the termination of paroxysmal atrial fibrillation in humans," *Europace*, vol. 9, no. 7, pp. 466–470, 2007.

[95] R. Alcaraz and J. J. Rieta, "Sample entropy of the main atrial wave predicts spontaneous termination of paroxysmal atrial fibrillation," *Med. Eng. Phys.*, vol. 31, no. 8, pp. 917–922, 2009.

[96] R. Alcaraz and J. J. Rieta, "The application of nonlinear metrics to assess organization differences in short recordings of paroxysmal and persistent atrial fibrillation," *Physiol. Meas.*, vol. 31, no. 1, p. 115, 2009.

[97] R. Alcaraz, F. Sandberg, L. Sörnmo, and J. J. Rieta, "Classification of paroxysmal and persistent atrial fibrillation in ambulatory ECG recordings," *IEEE Trans. Biomed. Eng.*, vol. 58, no. 5, pp. 1441–1449, 2011.

[98] M. Meo, V. Zarzoso, O. Meste, D. G. Latcu, and N. Saoudi, "Catheter ablation outcome prediction in persistent atrial fibrillation using weighted principal component analysis," *Biomed. Signal Process. Control*, vol. 8, no. 6, pp. 958–968, 2013.

[99] M. Meo, V. Zarzoso, O. Meste, D. G. Latcu, and N. Saoudi, "Spatial variability of the 12-lead surface ECG as a tool for noninvasive prediction of catheter ablation outcome in persistent atrial fibrillation," *IEEE Trans. Biomed. Eng.*, vol. 60, no. 1, pp. 20–27, 2013.

[100] L. Y. Di Marco, D. Raine, J. P. Bourke, and P. Langley, "Recurring patterns of atrial fibrillation in surface ECG predict restoration of sinus rhythm by catheter ablation," *Comput. Biol. Med.*, vol. 54, pp. 172–179, 2014.

[101] R. Alcaraz, F. Hornero, and J. J. Rieta, "Electrocardiographic spectral features for long-term outcome prognosis of atrial fibrillation catheter ablation," *Ann. Biomed. Eng.*, vol. 44, no. 11, pp. 3307–3318, 2016.

[102] T. Lankveld, S. Zeemering, D. Scherr, P. Kuklik, B. A. Hoffmann, S. Willems, B. Pieske, M. Haïssaguerre, P. Jaïs, H. J. Crijns, and U. Schotten, "Atrial fibrillation complexity parameters derived from surface ECGs predict procedural outcome and long-term follow-up of stepwise catheter ablation for atrial fibrillation," *Circ. Arrhythm. Electrophysiol.*, vol. 9, no. 2, p. e003354, 2016.

[103] V. Zarzoso, D. G. Latcu, A. R. Hidalgo-Muñoz, M. Meo, O. Meste, I. Popescu, and N. Saoudi, "Non-invasive prediction of catheter ablation outcome in persistent atrial fibrillation by fibrillatory wave amplitude computation in multiple electrocardiogram leads," *Arch. Cardiovasc. Dis.*, vol. 109, no. 12, pp. 679–688, 2016.

[104] A. R. Hidalgo-Muñoz, D. G. Latcu, M. Meo, O. Meste, I. Popescu, N. Saoudi, and V. Zarzoso, "Spectral and spatiotemporal variability ECG parameters linked to catheter ablation outcome in persistent atrial fibrillation," *Comput. Biol. Med.*, vol. 88, pp. 126–131, 2017.

[105] V. P. Raygor, J. Ng, and J. J. Goldberger, "Surface ECG f wave analysis of dofetilide drug effect in the atrium," *J. Cardiovasc. Electrophysiol.*, vol. 26, no. 6, pp. 644–648, 2015.

[106] M. Aunes, K. Egstrup, L. Frison, A. Berggren, M. Stridh, L. Sörnmo, and N. Edvardsson, "Rapid slowing of the atrial fibrillatory rate after administration of AZD7009 predicts conversion of atrial fibrillation," *J. Electrocardiol.*, vol. 47, no. 3, pp. 316–323, 2014.

[107] E. W. Black-Maier, S. D. Pokorney, A. S. Barnett, P. Liu, P. Shrader, J. Ng, J. J. Goldberger, W. Zareba, J. P. Daubert, A. O. Grant, *et al.*, "Ranolazine reduces atrial fibrillatory wave frequency," *Europace*, vol. 19, no. 7, pp. 1096–1100, 2017.

[108] S. Petrutiu, J. Ng, G. M. Nijm, H. Al-Angari, S. Swiryn, and A. V. Sahakian, "Atrial fibrillation and waveform characterization," *IEEE Eng. Med. Biol. Mag.*, vol. 25, no. 6, pp. 24–30, 2006.

[109] K. T. Konings, C. J. Kirchhof, J. R. Smeets, H. J. Wellens, O. C. Penn, and M. A. Allessie, "High-density mapping of electrically induced atrial fibrillation in humans.," *Circulation*, vol. 89, no. 4, pp. 1665–1680, 1994.

[110] A. Harada, K. Sasaki, T. Fukushima, M. Ikeshita, T. Asano, S. Yamauchi, S. Tanaka, and T. Shoji, "Atrial activation during chronic atrial fibrillation in patients with isolated mitral valve disease," *Ann. Thorac. Surg.*, vol. 61, no. 1, pp. 104–112, 1996.

[111] M. Holm, S. Pehrson, M. Ingemansson, L. Sörnmo, R. Johansson, L. Sandhall, M. Sunemark, B. Smideberg, C. Olsson, and S. B. Olsson, "Non-invasive assessment of the atrial cycle length during atrial fibrillation in man: introducing, validating and illustrating a new ECG method," *Cardiovasc. Res.*, vol. 38, no. 1, pp. 69–81, 1998.

[112] A. Buttu, E. Pruvot, J. Van Zaen, A. Viso, A. Forclaz, P. Pascale, S. M. Narayan, and J.-M. Vesin, "Adaptive frequency tracking of the baseline ecg identifies the site of atrial fibrillation termination by catheter ablation," *Biomed. Signal Process. Control*, vol. 8, no. 6, pp. 969–980, 2013.

[113] F. Sandberg, M. Stridh, and L. Sörnmo, "Frequency tracking of atrial fibrillation using hidden Markov models," *IEEE Trans. Biomed. Eng.*, vol. 55, no. 2, pp. 502–511, 2008.

[114] S. Petrutiu, A. V. Sahakian, and S. Swiryn, "Short-term dynamics in fibrillatory wave characteristics at the onset of paroxysmal atrial fibrillation in humans," *J. Electrocardiol.*, vol. 40, no. 2, pp. 155–160, 2007.

[115] M. Thurmann and J. G. Janney JR, "The diagnostic importance of fibrillatory wave size," *Circulation*, vol. 25, no. 6, pp. 991–994, 1962.

[116] M. R. Culler, J. A. Boone, and P. C. Gazes, "Fibrillatory wave size as a clue to etiological diagnosis.," *Am. Heart J.*, vol. 66, pp. 435–436, 1963.

[117] H. Åberg, "Atrial fibrillation: II. A study of fibrillatory wave size on the regular scalar electrocardiogram," *Acta Med. Scand.*, vol. 185, no. 1-6, pp. 381–385, 1969.

[118] I. Nault, N. Lellouche, S. Matsuo, S. Knecht, M. Wright, K.-T. Lim, F. Sacher, P. Platonov, A. Deplagne, P. Bordachar, N. Derval, M. D. O̸Neill, G. J. Klein, M. Hocini, P. Jaïs, J. Clémenty, and M. Haïssaguerre, "Clinical value of fibrillatory wave amplitude on surface ECG in patients with persistent atrial fibrillation," *J. Interv. Card. Electrophysiol.*, vol. 26, no. 1, pp. 11–19, 2009.

[119] B. Mutlu, M. Karabulut, E. Eroglu, K. Tigen, F. Bayrak, H. Fotbolcu, and Y. Basaran, "Fibrillatory wave amplitude as a marker of left atrial and left atrial appendage function, and a predictor of thromboembolic risk in patients with rheumatic mitral stenosis," *Int. J. Cardiol.*, vol. 91, no. 2-3, pp. 179–186, 2003.

[120] Q. Xi, A. V. Sahakian, J. Ng, and S. Swiryn, "Atrial fibrillatory wave characteristics on surface electrogram: ECG to ECG repeatability over twenty-four hours in clinically stable patients," *J. Cardiovasc. Electrophysiol.*, vol. 15, no. 8, pp. 911–917, 2004.

[121] Q. Xi, A. V. Sahakian, T. G. Frohlich, J. Ng, and S. Swiryn, "Relationship between pattern of occurrence of atrial fibrillation and surface electrocardiographic fibrillatory wave characteristics," *Heart Rhythm*, vol. 1, no. 6, pp. 656–663, 2004.

[122] R. Alcaraz, F. Hornero, and J. J. Rieta, "Noninvasive time and frequency predictors of long-standing atrial fibrillation early recurrence after electrical cardioversion," *Pacing Clin. Electrophysiol.*, vol. 34, no. 10, pp. 1241–1250, 2011.

[123] P. Bonizzi, S. Zeemering, J. M. Karel, L. Y. Di Marco, L. Uldry, J. Van Zaen, J.-M. Vesin, and U. Schotten, "Systematic comparison of non-invasive measures for the assessment of atrial fibrillation complexity: a step forward towards standardization of atrial fibrillation electrogram analysis," *Europace*, vol. 17, no. 2, pp. 318–325, 2015.

[124] R. Alcaraz and J. J. Rieta, "A review on sample entropy applications for the non-invasive analysis of atrial fibrillation electrocardiograms," *Biomed. Signal Process. Control*, vol. 5, no. 1, pp. 1–14, 2010.

[125] P. Bonizzi, M. de la Salud Guillem, A. M. Climent, J. Millet, V. Zarzoso, F. Castells, and O. Meste, "Noninvasive assessment of the complexity and stationarity of the atrial wavefront patterns during atrial fibrillation," *IEEE Trans. Biomed. Eng.*, vol. 57, no. 9, pp. 2147–2157, 2010.

[126] L. Y. Di Marco, J. P. Bourke, and P. Langley, "Spatial complexity and spectral distribution variability of atrial activity in surface ECG recordings of atrial fibrillation," *Med. Biol. Eng. Comput.*, vol. 50, no. 5, pp. 439–446, 2012.

[127] R. Alcaraz, F. Hornero, and J. J. Rieta, "Dynamic time warping applied to estimate atrial fibrillation temporal organization from the surface electrocardiogram," *Med. Eng. Phys.*, vol. 35, no. 9, pp. 1341–1348, 2013.

[128] T. A. Lankveld, S. Zeemering, H. J. Crijns, and U. Schotten, "The ECG as a tool to determine atrial fibrillation complexity," *Heart*, vol. 100, no. 14, pp. 1077–1084, 2014.

[129] R. Goya-Esteban, F. Sandberg, Ó. Barquero-Pérez, A. García-Alberola, L. Sörnmo, and J. L. Rojo-Álvarez, "Long-term characterization of persistent atrial fibrillation: wave morphology, frequency, and irregularity analysis," *Med. Biol. Eng. Comput.*, vol. 52, pp. 1053–1060, Dec 2014.

[130] T. H. Everett IV, J. R. Moorman, L.-C. Kok, J. G. Akar, and D. E. Haines, "Assessment of global atrial fibrillation organization to optimize timing of atrial defibrillation," *Circulation*, vol. 103, no. 23, pp. 2857–2861, 2001.

[131] T. H. Everett, L.-C. Kok, R. H. Vaughn, R. Moorman, and D. E. Haines, "Frequency domain algorithm for quantifying atrial fibrillation organization to increase defibrillation efficacy," *IEEE Trans. Biomed. Eng.*, vol. 48, no. 9, pp. 969–978, 2001.

[132] S. Babaeizadeh, R. E. Gregg, E. D. Helfenbein, J. M. Lindauer, and S. H. Zhou, "Improvements in atrial fibrillation detection for real-time monitoring," *J. Electrocardiol.*, vol. 42, no. 6, pp. 522–526, 2009.

[133] S. Ladavich and B. Ghoraani, "Rate-independent detection of atrial fibrillation by statistical modeling of atrial activity," *Biomed. Signal Process. Control*, vol. 18, pp. 274–281, 2015.

[134] J. Ródenas, M. García, R. Alcaraz, and J. J. Rieta, "Wavelet entropy automatically detects episodes of atrial fibrillation from single-lead electrocardiograms," *Entropy*, vol. 17, no. 9, pp. 6179–6199, 2015.

[135] L. Sörnmo, A. Petrėnas, and V. Marozas, "Detection of atrial fibrillation," in *Atrial Fibrillation from an Engineering Perspective*, pp. 73–135, Springer, 2018.

[136] Y. Xia, N. Wulan, K. Wang, and H. Zhang, "Detecting atrial fibrillation by deep convolutional neural networks," *Comp. Biol. Med.*, vol. 93, pp. 84–92, 2018.

[137] L. Sörnmo, A. Petrėnas, M. Henriksson, and V. Marozas, "Letter regarding the article "detecting atrial fibrillation by deep convolutional neural networks" by xia et al.," *Comp. Biol. Med.*, vol. 100, pp. 41–42, 2018.

[138] S. Asgari, A. Mehrnia, and M. Moussavi, "Automatic detection of atrial fibrillation using stationary wavelet transform and support vector machine," *Comp. Biol. Med.*, vol. 60, pp. 132–142, 2015.

[139] M. Haïssaguerre, P. Sanders, M. Hocini, L.-F. Hsu, D. C. Shah, C. Scavée, Y. Takahashi, M. Rotter, J.-L. Pasquié, S. Garrigue, J. Clémenty, and P. Jaïs, "Changes in atrial fibrillation cycle length and inducibility during catheter ablation and their relation to outcome," *Circulation*, vol. 109, no. 24, pp. 3007–3013, 2004.